Journal Pre-proof

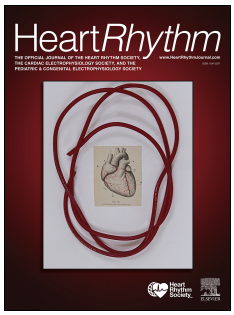

Non-invasive Assessment of HydroQUInidine EffecT in Brugada Syndrome (QUIET BrS)

Julia C. Isbister, MBBS, PhD, Marina Strocchi, PhD, Matthew Riedy, BAppSci (hons), Laura Yeates, BSc (hons), GradDipGenCouns, PhD, Belinda Gray, MBBS, PhD, Emma S. Singer, BMedSc, Richard D. Bagnall, PhD, Jodie Ingles, PhD, MPH, Hariharan Raju, MBChB PhD, Christopher Semsarian, MBBS, PhD, MPH, FHRS, Steven A. Niederer, PhD, Raymond W. Sy, MBBS, PhD

PII: S1547-5271(24)03659-2

DOI: https://doi.org/10.1016/j.hrthm.2024.12.014

Reference: HRTHM 10951

To appear in: *Heart Rhythm*

Received Date: 19 June 2024

Revised Date: 4 December 2024

Accepted Date: 9 December 2024

Please cite this article as: Isbister JC, Strocchi M, Riedy M, Yeates L, Gray B, Singer ES, Bagnall RD, Ingles J, Raju H, Semsarian C, Niederer SA, Sy RW, Non-invasive Assessment of HydroQUInidine EffecT in Brugada Syndrome (QUIET BrS), *Heart Rhythm* (2025), doi: https://doi.org/10.1016/j.hrthm.2024.12.014.

Non-invasive Assessment of Hydro**QUI**nidine **E**ffec**T** in **Br**ugada **S**yndrome (QUIET BrS)

Julia C Isbister MBBS, PhD [a,b], Marina Strocchi PhD [c,d], Matthew Riedy BAppSci (hons) [e], Laura Yeates BSc (hons), GradDipGenCouns, PhD [a,b,f,g], Belinda Gray MBBS, PhD [a,b], Emma S Singer BMedSc [a,f,h], Richard D Bagnall PhD [a,f,h], Jodie Ingles PhD, MPH [b,h], Hariharan Raju MBChB PhD [i], Christopher Semsarian MBBS, PhD, MPH, FHRS [a,b,f], Steven A Niederer PhD [c,d,j], Raymond W Sy MBBS, PhD [a,b]

[a] Faculty of Medicine and Health, University of Sydney, Australia.

[b] Department of Cardiology, Royal Prince Alfred Hospital, Australia.

[c] National Heart and Lung Institute, Imperial College London, United Kingdom.

[d] School of Biomedical Engineering and Imaging Sciences, King's College London, United Kingdom

[e] Medtronic Australasia

[f] Agnes Ginges Centre for Molecular Cardiology at Centenary Institute, The University of Sydney, Australia.

[g] Genomics and Inherited Disease Program, Garvan Institute of Medical Research, and University of New South Wales, Australia

[h] Bioinformatics and Molecular Genetics Group at Centenary Institute, The University of Sydney, Australia.

[i] Faculty of Medicine, Health and Human Sciences, Macquarie University, Australia.

[j] The Alan Turing Institute, United Kingdom

Word Count = 5847

Short title: Electrophysiological effects of Hydroquinidine in Brugada Syndrome

Disclosures: Medtronic Australasia Pty Ltd provided limited equipment and technical assistance under an External Research Program grant (#ERP-2020-12429). Mr Matthew Riedy is an employee of Medtronic Australasia Pty Ltd.

Article type: *Original Clinical Research*

Address for Correspondence
Associate Professor Raymond Sy
Department of Cardiology
Royal Prince Alfred Hospital
Email: raymond.sy01@gmail.com

ABSTRACT

Background: Hydroquinidine reduces arrhythmic events in patients with Brugada syndrome (BrS). The mechanism by which it exerts antiarrhythmic benefit and its electrophysiological effects on BrS substrate remain incompletely understood.

Objective: This study aimed to determine the effect of Hydroquinidine on ventricular depolarisation and repolarisation in patients with BrS *in vivo*.

Methods: Twelve patients with BrS underwent electrocardiogram (standard, high-lead and signal averaged) and electrocardiographic imaging (ECGi) at baseline and "on-treatment" with Hydroquinidine 300mg twice daily. ST-segment elevation, activation time (AT), repolarisation time (RT) and activation-recovery intervals (ARI) were computed for the ventricles and the right ventricular outflow tract (RVOT). Serum Hydroquinidine levels were determined, and adverse drug events captured through medication survey.

Results: Hydroquinidine increased RT (301.1 ± 24.1ms vs 348.8 ± 28.3ms, p <0.001), repolarisation gradients (1.1 ± 0.4 ms/mm vs 1.6 ± 0.4 ms/mm, p<0.001) and ARI (241.3 ± 18.1 ms vs 284.8 ± 21.5 ms, p<0.001) in the RVOT, with a greater change in the RVOT compared to the rest of the ventricles. In contrast, activation parameters did not change significantly on-treatment with Hydroquinidine, although there was a subtle increase in ST-segment elevation over the RVOT (1.5 ± 0.7mV vs 1.8 ± 0.8mV; P<0.001). Hydroquinidine levels did not correlate with electrophysiological changes or occurrence of adverse drug reactions. One patient developed frequent non-sustained ventricular tachycardia on-treatment with Hydroquinidine.

Conclusions: Hydroquinidine primarily effects ventricular repolarisation and action potential duration (indicated by ARI) in patients with BrS and demonstrates regional variation with more significant changes in the RVOT.

KEYWORDS:

Brugada syndrome, Hydroquinidine, electrocardiographic imaging, non-invasive, ventricular activation, ventricular repolarisation, activation-recovery interval.

INTRODUCTION

Quinidine (in its various formulations, including Hydroquinidine) has been shown to reduce the inducibility of arrhythmia on programmed stimulation and the frequency of clinical ventricular arrhythmias in patients with Brugada syndrome (BrS).[1-3] Despite challenges with access[3] and poor tolerance due to side effects[1, 4], it is the only medication recommended for long-term reduction of arrhythmic events in BrS.[5] However, the specific mechanism by which Quinidine reduces arrhythmia in BrS remains incompletely understood.

The mechanistic uncertainty around Quinidine's antiarrhythmic effects in BrS parallels ongoing debate regarding the underlying pathophysiology of the condition itself, which centres around two main hypotheses. The abnormal depolarisation hypothesis, supported by fractionated local electrograms frequently observed in the RVOT of patients with BrS, holds that intermittent activation failure and resultant unidirectional block provides substrate for arrhythmia.[6-8] The repolarisation hypothesis asserts that accentuation of the already prominent phase 1 notch in RVOT epicardial myocytes, through a reduction in I_{Na} and/or increase in I_{To}, shortens the epicardial action potential, setting up a transmural gradient and a propensity for phase 2 re-entry and ventricular arrhythmia.[9, 10] While there has been a degree of convergence between these two hypotheses, the relative contributions of depolarisation and repolarisation abnormalities remain unclear.

Early identification of Quinidine's inhibition of the inward sodium current (I_{Na}) led to its classification as a class 1 antiarrhythmic agent, but it also inhibits the transient outward current (I_{To}) and delayed rectifier current (I_{Kr}).[11-14] Heterogeneity of its effect across the

epicardium and endocardium has also been described.[15] *In vivo,* Quinidine prolongs action potential duration, repolarisation and refractory periods in healthy subjects[13, 16] and has been reported to variably attenuate ST elevation in BrS.[2, 4, 17] Investigations into its mechanism as an antiarrhythmic agent in BrS have largely been based on models related to the 'repolarisation hypothesis'.[9] Importantly, the potential effects of Quinidine on depolarisation in BrS have not been systematically reported and regional variations in its effect in the RVOT compared to the rest of the ventricles have not been systematically studied.

The aim of this study was to investigate the *in vivo* electrophysiological effects of Hydroquinidine in patients with BrS using non-invasive evaluation including electrocardiographic imaging (ECGi).

METHODS

Patient selection

Study participants were recruited from the Genetic Heart Disease clinic at Royal Prince Alfred Hospital, Sydney, Australia between 2019 and 2021. Patients were invited to participate if they were over 18 years of age, not taking Quinidine at the time of enrolment, and had either a spontaneous type 1 Brugada ECG pattern, or history of cardiac arrest with drug-induced type 1 Brugada ECG pattern. Exclusion criteria can be found in **Supplemental Methods**. This study was approved by the Sydney local health district human research committee (X19-0258), registered with the Australian New Zealand Clinical Trials Registry (ACTRN 12620000934943) and all patients provided written informed consent to participate.

Study Protocol

The study protocol is shown in **Supplemental Figure 1**. Participants received sustained release Hydroquinidine (Hydroquinidine hydrochloride, *Serecor* 300mg capsules, Sanofi-Aventis, Paris, France) 300mg twice daily for 14±7 days to reach steady state prior to "on-treatment" assessment. Serum Hydroquinidine levels were determined at the on-treatment visit with levels from 3 to 6µmol/L considered to be in the therapeutic range.[4] Baseline and on-treatment assessments were performed at the same time of day (morning) to minimise potential confounding from diurnal variability.

Standard and high praecordial lead 12-lead electrocardiograms (ECG) and signal-averaged ECG (SAECG) were performed at baseline and on-treatment assessments. Non-invasive electroanatomical mapping was performed at baseline and on-treatment assessments using

ECG imaging (ECGi). Participants completed a medication survey at the time of the on-treatment visit to monitor for medication adherence and side effects. Holter monitors were performed at baseline and on-treatment given the potential for proarrhythmia with Hydroquinidine and a prior report of non-sustained monomorphic VT on therapy.[2] All patients underwent genetic testing of *SCN5A* and variants were classified according to American College of Medical Genetics and Genomics (ACMG) criteria. Patients with pathogenic or likely pathogenic variants were considered *SCN5A* (+).

ECG Imaging using CardioInsight™

ECGi was performed using the CardioInsight™ non-invasive 3-dimensional mapping system (Medtronic Inc, Minneapolis, MN). ECGi methodology has been reported previously and is described in detail in supplementary data.[18, 19] Briefly, mapping was performed in sinus rhythm. Manual segmentation of ventricular anatomy from contrast computed tomography scans was performed and integrated with body surface signals. ST-segment elevation, activation times (AT), repolarisation times (RT corrected for heart rate) and activation-recovery interval (ARI where ARI = RT- AT) were computed using previously reported methods and details can be found in **Supplemental Methods**.[7, 20] Isochronal electroanatomical maps were created from computed values. Global activation gradients and repolarisation gradients as well as EGM T-wave width and amplitude were computed for the entire ventricles. The pathological changes in BrS are thought to be localised to the RVOT and thus regional analysis of metrics was performed to examine the electrophysiological properties of the biventricular mass excluding the RVOT (BiV) and RVOT.[6, 7] Mean AT in the areas of late activation (later than 80ms) was also calculated as described previously.[7]

Statistics

GraphPad Prism Version 9.1.2 (GraphPad Software, San Diego, California USA) was used for statistical analysis. Descriptive statistics were used to determine the characteristics of the cohort with continuous variables reported as means and standard deviations and categorical variables as counts and percentages of available data. Continuous variables were compared using paired Student t-tests. Statistical significance was defined as p-value <0.05.

RESULTS

Cohort characteristics

The clinical characteristics of the cohort are reported in **Table 1**. Eleven of 12 participants (91.7%) were male, and the mean age was 47.6 ± 10.9 years. All participants had a documented spontaneous type 1 BrS pattern ECG, except for one cardiac arrest survivor who had an inducible type 1 ECG following Ajmaline challenge. Three patients had survived cardiac arrest while two had a history of syncope of unclear aetiology. Two patients had frameshift variants in *SCN5A* (p.Glu955Aspfs*74 and p.Gln646Argfs*5) which were classified as likely pathogenic or pathogenic, respectively. Other patients did not have suspicious variants in *SCN5A*.

ECG Parameters

On-treatment, there was a significant increase in corrected QT interval (369.5msec vs 434.8msec, p<0.0001) as well as a smaller but statistically significant increase in QRS duration (110.7msec vs 117.8msec, p=0.004). Seven of 11 (63.6%) patients (the patient with baseline right bundle branch block was excluded from SAECG analysis) had late potentials on SAECG (as previously defined [21]) at baseline. One of these patients did not have late potentials on-treatment, while another patient developed late potentials on-treatment. There were no significant changes in other ECG or signal-averaged ECG parameters on-treatment (**Table 2**).

ECGi Parameters: ST-segment elevation

At baseline, there was significantly greater ST-segment elevation in the RVOT compared to the BiV (1.5 ± 0.7mV vs 0.4 ± 0.1mV, p< 0.001) (**Table 2 and Figure 1A**). Compared to baseline, treatment with hydroquinidine resulted in a small but statistically significant increase in ST-

segment elevation in the RVOT (1.5 ± 0.7mV at baseline vs 1.8 ± 0.8mV on-treatment; P<0.001; mean change 0.3mV, range 0.1-0.7mV) but no change was seen in the ST-segment potential in the BiV mass (**Table 2 and Figure 1B**).

ECGi Parameters: ventricular activation

Baseline activation maps showed a consistent area of delayed activation in the RVOT in all participants (representative maps shown in **Figure 2A**). Mean AT was longer and activation gradients were twice as steep in the RVOT compared to the BiV at baseline (**Table 2**). Activation gradient maps suggested that late activation in the RVOT was due to an area of steep deceleration of the activation wavefront in the border zones of the RVOT rather than progressive delay throughout the RVOT (**Figure 2A**).

There was no significant change in activation pattern or global activation parameters in response to Hydroquinidine, with mean AT and activation gradients in RVOT and BiV unchanged on-treatment (**Figure 2B** and **Table 2**). There was a statistically significant increase in mean AT in areas of late activation (**Table 2**), but this effect was largely driven by 3 outliers (one patient with RBBB and two *SCN5A* (+) patients, discussed below). Morphology and degree of fractionation of low-amplitude electrograms from areas of late activation in the RVOT were similar between baseline and on-treatment assessments **(Supplemental Figure 2)**. Ventricular activation was similar between patients with therapeutic and sub-therapeutic Hydroquinidine levels (**Supplemental Table 1**).

ECGi Parameters: ventricular repolarisation

At baseline, mean RT was longer in the RVOT than BiV (301.1 ± 24.1 vs 258.2 ± 18.2, p <0.001). There were marked changes in ventricular repolarisation in response to Hydroquinidine (**Figure 3**). Mean RT prolonged in the RVOT and the BiV, with a proportionally greater increase in the RVOT than the BiV on-treatment (mean difference in RT RVOT – BiV, 42.9 ± 10.6 vs 66.0 ± 13.0, p <0.001) (**Table 2**). The repolarisation gradient increased in both the RVOT and BiV (RVOT: 1.1 ± 0.4 vs 1.6 ± 0.4, p<0.001, BiV:1.2 ± 0.4 vs 1.9 ± 0.5, p<0.001), **Table 2**. EGM T-wave amplitude decreased, and T-wave width increased throughout the myocardium on-treatment (**Table 2** and **Supplemental Figure 3**). Changes in ventricular repolarisation in response to Hydroquinidine were independent of serum Hydroquinidine levels (**Supplemental Table 1**).

ECGi Parameters: activation-recovery interval

Activation-recovery interval, a surrogate for local action potential duration, prolonged with Hydroquinidine (**Figure 4**), with a proportionally greater lengthening in the RVOT (mean ARI RVOT-BiV 17.2 ± 9.1ms vs 37.9 ± 12.6ms p=0.001, **Table 2**). Changes in mean ARI with Hydroquinidine were independent of serum Hydroquinidine levels. (**Supplemental Table 1**).

Serum Hydroquinidine levels and side effects of therapy

Five patients (42%) had therapeutic serum Hydroquinidine levels on-treatment. Mean serum Hydroquinidine level was 3.0 ± 1.0µmol/L (range 1.3-4.7µmol/L). Eight out of 12 (75%) participants reported a suspected side effect, most commonly, diarrhoea (n=5). No significant difference in serum Hydroquinidine level was detected between those who experienced side effects and those who did not (2.9µmol vs 3.1µmol, p=0.790). No patients discontinued

Hydroquinidine due to side effects. No clinically significant blood dyscrasias or impairment of liver function occurred on-treatment.

SCN5A positive patients

One patient (BEU6) developed frequent, non-sustained monomorphic ventricular tachycardia originating from the RVOT on-treatment, detected on Holter monitoring (**Figure 5**). The patient was asymptomatic with serum Hydroquinidine level of 2.87 µmol/L and QTc was 429ms. BEU6 was one of 2 patients with a pathogenic frameshift variant in *SCN5A*. Surface ECGs from Holter recording and ECGi maps of patient BEU6 are shown in **Figure 5**. When compared to the mean response in the cohort, BEU6 exhibited a greater increase in the activation gradient with Hydroquinidine therapy (0.8ms/mm at baseline; 1.5ms/mm on-treatment) and mean AT in the area of late activation also increased to a greater extent during Hydroquinidine (86.5ms at baseline; 120ms on-treatment). Interestingly, a similar pattern was also seen in the other patient with a pathogenic variant in *SCN5A*, but no arrhythmia observed on Holter. (**Figure 6**). In contrast, the effect of Hydroquinidine on ST-segment elevation and repolarisation parameters was similar in *SCN5A* (+) patients compared to *SCN5A* (-) patients.

DISCUSSION

This study sheds new light on the *in vivo* electrophysiological characteristics of patients with BrS, and the effects of Hydroquinidine. The key findings were as follows: 1) there is significant slowing of activation and repolarisation as well as prolongation of ARI at the border zone of the RVOT in BrS; 2) Hydroquinidine does not significantly alter myocardial activation in the RVOT or more generally in the ventricles but a subtle increase in ST-segment elevation was observed in RVOT during treatment; 3) Hydroquinidine prolongs action potential duration (APD) evidenced by an increase in ARI; 4) the RVOT exhibited a greater increase in repolarisation on Hydroquinidine compared to the rest of the ventricles; 5) similar electrophysiological changes and frequency of side effects were observed in patients with 'sub-therapeutic' and 'therapeutic' drug levels.

Imbalance between depolarisation and repolarisation in the RVOT in BrS

Our data confirm delayed activation in the RVOT, similar to that described in previous BrS cohorts.[18, 22] Isochronal crowding on activation maps and steep increase in activation gradient suggest marked deceleration in the activation wavefront between the RV body and RVOT, rather than homogenous delay throughout the RVOT. Significant ST-segment elevation was also confined to the RVOT, consistent with previous studies using isolated human hearts, computer models and epicardial mapping that have indicated that the ST-segment elevation in electrograms over the RVOT may be caused by local excitation failure in the subepicardium.[7, 23] Interestingly, ARI maps also reveal a band of increased ARI and region of steep repolarisation gradients at the border of the RVOT in this cohort. In normal myocardium, ARI is inversely proportional to activation time (ARI = RT – AT) resulting in

relative regional homogeneity of repolarisation times.[24] An increase in ARI reveals an imbalance between activation and repolarisation with a proportionally greater delay in repolarisation than depolarisation. This band-like region of increased ARI and steep repolarisation gradients was noted to be a distinguishing feature in patients with BrS from those with RBBB previously.[18] Given fibrosis is well described in BrS [25], it is notable that ARI prolongation and dispersion of repolarisation have also been demonstrated in scar border zones of patients without BrS and variations in scar location between myocardial layers results in transmural heterogeneity of APD, and may be important in arrhythmogenesis.[26]

Modulation of repolarisation by Quinidine is a potential antiarrhythmic mechanism in BrS

Although it could be expected that Quinidine's inhibition of the sodium current may exacerbate any pre-existing impairment of myocardial activation (especially in the RVOT), inhibition of I_{To} by Quinidine may increase the source current and actually prevent activation failure, staving off the unidirectional block that causes arrhythmia.[27] In the present study, there was a small but statistically significant increase in the ST-segment potential (mean 0.3mV) in the RVOT electrograms during treatment with Hydroquinidine, but there was no significant change in regional (RVOT) or global activation time in response to Hydroquinidine on ECGi. ST-segment elevation in the RVOT is exacerbated by sodium-channel blocking agents such as Ajmaline and this has been demonstrated to be due to epicardial excitation failure.[7] Hence, it is plausible that Hydroquinidine may also have a subtle effect on transmural activation to account for the small increase in ST-segment potential over the RVOT during treatment. However, this may not have been sufficient to affect regional RVOT activation times. In contrast, our data show a generalised increase in ARI and RT with Hydroquinidine. Prolongation of the APD (observed here as increased ARI) increases the effective refractory

248 period (ERP) of tissue and may reduce susceptibility to re-entry. Moreover, changes in APD
249 and RT also demonstrated regional variation, with proportionally greater on-treatment effect
250 in the RVOT compared to the rest of the ventricles. This is particularly noteworthy given the
251 RVOT has been shown to be the region of arrhythmia initiation in BrS.[28, 29] It is possible that
252 regional variations in the effect of Hydroquinidine contribute to its specific benefits in BrS.
253 This hypothesis is supported by a previous study showing significantly shorter RVOT-ERP and
254 RVOT-APD in patients with BrS compared to control patients, and correction of the RVOT-APD
255 with Quinidine therapy, resulting in reduced VF inducibility.[30] Based on these observations,
256 we speculate that the antiarrhythmic effect of Quinidine in BrS may be primarily due to
257 modulation of repolarisation, especially in the RVOT.
258
259 *Drug monitoring and adverse effects*
260 We did not observe a difference in electrophysiological effect between patients with
261 therapeutic serum Hydroquinidine levels and patients with subtherapeutic Hydroquinidine
262 levels. While the absence of statistically significant difference should be interpreted with
263 caution given the small numbers in this study, it is interesting to note that this finding parallels
264 a previous report that serum drug level was similar between patients rendered non-inducible
265 with Hydroquinidine and those who had persistent inducibility of arrhythmia on therapy (2.7
266 ± 1.3 µmol/l vs 2.8 ± 1.6 µmol/l).[2] Notably, the mean serum levels in both groups fell below
267 the traditional "therapeutic range" of Hydroquinidine (3 to 6µmol/L).[2, 4] While it is possible
268 that the electrophysiological effects of Hydroquinidine and/or suppression of inducible
269 arrhythmia are truly not linked to serum drug level, a more likely explanation is that
270 Hydroquinidine exerts antiarrhythmic effects at lower does that traditionally expected. This
271 notion is supported by observational studies but ideally it should be validated with

prospective studies specifically evaluating the effects of different dosing.[31, 32] Despite the relatively low dose of Hydroquinidine used in this study, two thirds of patients experienced side effects attributed to the drug, unrelated to serum level. Hence, monitoring serum Hydroquinidine levels does not appear to correlate with efficacy or safety, and we agree with previous authors that QTc is a simple but valuable marker of adherence to therapy.[2]

The development of monomorphic ventricular tachycardia during Hydroquinidine therapy in patient BEU6 was a concerning finding. The ventricular tachycardia was likely attributable to Hydroquinidine given the absence of any arrhythmia at baseline and high burden on treatment. Monomorphic ventricular tachycardia has been described in BrS in the absence of Quinidine therapy but Quinidine has also been associated with proarrhythmia.[2, 4, 33] Importantly, Quinidine's prolongation of the QT interval only rarely appears to be associated with proarrhythmia.[1, 2, 4, 34] Indeed, QTc was normal and the effect of Hydroquinidine on repolarisation parameters in BEU6 were comparable to the rest of the cohort. However, there was an increase in the activation gradient in the border-zone of the RVOT and mean activation in the region of latest activation with Hydroquinidine therapy was quite different to the rest of the cohort. One may speculate that these changes on Hydroquinidine may predispose to re-entrant arrhythmia from the RVOT.

Interestingly, the effect of Hydroquinidine on activation in the RVOT appeared to be more apparent in patients with disease-causing *SCN5A* variants, whereas this was either absent or less marked in patients without any deleterious variants in *SCN5A*. It is possible that patients with functionally abnormal cardiac sodium channel may have an altered response to the effects of Quinidine, for example, being more sensitive to the inhibition of the I_{Na}. Our

296 findings, albeit in only two patients, parallel the observations of Pannone et al, who showed
297 greater delay in AT in the RVOT with Ajmaline in *SCN5A* (+) patients compared to *SCN5A* (-)
298 patients.[35] The impact of genotype on differential effects of Hydroquinidine in BrS warrants
299 further exploration.

LIMITATIONS

The number of subjects in this pilot study was low and thus adjustment for differences in demographic characteristics, clinical presentation and genotype was not possible in the evaluation of electrophysiological effects of Hydroquinidine. ECGi records body surface potentials and then uses an inverse problem to reconstruct unipolar electrograms of transmural electrical activity on an epicardial shell. ECGi does not distinguish which myocardial layer predominately contributes to the signal.[36] Thus, while abnormal substrate with delayed activation and ST-segment elevation were clearly demonstrated in the RVOT in our cohort, the transmural heterogeneity and specific epicardial or endocardial effects of Hydroquinidine could not be assessed. While such differences are best studied with combined epicardial and endocardial mapping (eg. in patients undergoing catheter ablation), a slightly 'less invasive' approach for evaluation in future studies may be simultaneous endocardial mapping and ECGi with signal subtraction to model transmural electrical gradients. ECGi analysis is also limited by its spatial resolution (**Supplemental Table 2**), and there are inherent challenges with studying heterogeneities on a submillimeter level using currently available clinical mapping techniques. Nevertheless, the current study demonstrates that non-invasive mapping may have a role in evaluating and monitoring the effect of drug therapy in BrS.

Segmentation of the RVOT was based on anatomical landmarks, and this may not mirror the extent of the abnormal 'electrical substrate' in the RVOT in BrS patients, leading to potential errors in comparative analysis of regional activity in the RVOT. The dose of the Hydroquinidine was relatively low (but similar to previous clinical studies); hence, future studies investigating *in vivo* effects at different doses would be useful given that different ion channel effects may

be observed at higher doses.[14] Furthermore, serum drug levels may not accurately reflect cellular drug concentrations.

CONCLUSION

The dominant electrophysiological effect of Hydroquinidine in patients with BrS is alteration of ventricular repolarisation, evidence by prolongation of RT and APD. These changes could explain the antiarrhythmic effect of Hydroquinidine observed in BrS. Further investigation is required to determine any transmural differences, as well as other potential modifiers of effect such as drug-dosing and disease-causing variants in *SCN5A*.

FUNDING:

This study was supported by Heart Foundation Vanguard Grant (#103082). Medtronic Australasia Pty Ltd provided CardioInsight workstation and technical assistance under External Research Program grant (#ERP-2020-12429). MS supported by NIHR Imperial Biomedical Research Centre (BRC) and British Heart Foundation Centre of Research Excellence (RE/18/4/34215). LY is the recipient of a co-funded National Heart Foundation of Australia/ National Health and Medical Research Council (NHMRC) PhD Scholarship (#102568/#191351). BG is the recipient of a Heart Foundation Future Leader Fellowship (#107244). RB is the recipient of a New South Wales Health Cardiovascular Disease Senior Scientist Grant. JI is the recipient of a National Heart Foundation of Australia Future Leader Fellowship (#106732). CS is the recipient of a National Health and Medical Research Council (NHMRC) Investigator Grant (#2016822) and a New South Wales Health Cardiovascular Disease Clinician Scientist Grant.

ACKNOWLEDGEMENTS

The authors of this manuscript would like to acknowledge Lorraine Mackenzie, University of South Australia, for determining serum Hydroquinidine levels for the study.

REFERENCES:

1. Belhassen B, Rahkovich M, Michowitz Y, Glick A, Viskin S. Management of Brugada Syndrome: Thirty-Three-Year Experience Using Electrophysiologically Guided Therapy With Class 1A Antiarrhythmic Drugs. Circ Arrhythm Electrophysiol Dec 2015;8:1393-1402.

2. Hermida JS, Denjoy I, Clerc J, Extramiana F, Jarry G, Milliez P, Guicheney P, Di Fusco S, Rey JL, Cauchemez B, Leenhardt A. Hydroquinidine therapy in Brugada syndrome. J Am Coll Cardiol May 19 2004;43:1853-1860.

3. Malhi N, Cheung CC, Deif B, et al. Challenge and Impact of Quinidine Access in Sudden Death Syndromes: A National Experience. JACC Clin Electrophysiol Mar 2019;5:376-382.

4. Andorin A, Gourraud JB, Mansourati J, et al. The QUIDAM study: Hydroquinidine therapy for the management of Brugada syndrome patients at high arrhythmic risk. Heart Rhythm Aug 2017;14:1147-1154.

5. Zeppenfeld K, Tfelt-Hansen J, de Riva M, et al. 2022 ESC Guidelines for the management of patients with ventricular arrhythmias and the prevention of sudden cardiac death. Eur Heart J Oct 21 2022;43:3997-4126.

6. Pieroni M, Notarstefano P, Oliva A, et al. Electroanatomic and Pathologic Right Ventricular Outflow Tract Abnormalities in Patients With Brugada Syndrome. J Am Coll Cardiol Dec 4 2018;72:2747-2757.

7. Nademanee K, Veerakul G, Nogami A, Lou Q, Hocini M, Coronel R, Behr ER, Wilde A, Boukens BJ, Haissaguerre M. Mechanism of the effects of sodium channel blockade on the arrhythmogenic substrate of Brugada syndrome. Heart Rhythm Mar 2022;19:407-416.

8. Haissaguerre M, Nademanee K, Sacher F, Cheniti G, Hocini M, Surget E, Dubois R, Vigmond E, Bernus O. Multisite conduction block in the epicardial substrate of Brugada syndrome. Heart Rhythm Mar 2022;19:417-426.

9. Yan GX, Antzelevitch C. Cellular basis for the Brugada syndrome and other mechanisms of arrhythmogenesis associated with ST-segment elevation. Circulation Oct 12 1999;100:1660-1666.

10. Szel T, Antzelevitch C. Abnormal repolarization as the basis for late potentials and fractionated electrograms recorded from epicardium in experimental models of Brugada syndrome. J Am Coll Cardiol May 20 2014;63:2037-2045.

11. Lee KS, Hume JR, Giles W, Brown AM. Sodium current depression by lidocaine and quinidine in isolated ventricular cells. Nature May 28 1981;291:325-327.

12. Imaizumi Y, Giles WR. Quinidine-induced inhibition of transient outward current in cardiac muscle. Am J Physiol Sep 1987;253:H704-708.

13. Vicente J, Johannesen L, Mason JW, Crumb WJ, Pueyo E, Stockbridge N, Strauss DG. Comprehensive T wave morphology assessment in a randomized clinical study of dofetilide, quinidine, ranolazine, and verapamil. J Am Heart Assoc Apr 13 2015;4:1-13.

14. Wu L, Guo D, Li H, Hackett J, Yan GX, Jiao Z, Antzelevitch C, Shryock JC, Belardinelli L. Role of late sodium current in modulating the proarrhythmic and antiarrhythmic effects of quinidine. Heart Rhythm Dec 2008;5:1726-1734.

15. Sosunov EA, Anyukhovsky EP, Rosen MR. Effects of quinidine on repolarization in canine epicardium, midmyocardium, and endocardium: I. In vitro study. Circulation Dec 2 1997;96:4011-4018.

16. Nademanee K, Stevenson WG, Weiss JN, Frame VB, Antimisiaris MG, Suithichaiyakul T, Pruitt CM. Frequency-dependent effects of quinidine on the ventricular action potential and QRS duration in humans. Circulation Mar 1990;81:790-796.

17. Watanabe H, Chinushi M, Washizuka T, Sugiura H, Hirono T, Komura S, Hosaka Y, Yamaura M, Tanabe Y, Furushima H, Fujita S, Aizawa Y. Variable electrocardiographic effects of short-term quinidine sulfate administration in Brugada syndrome. Pacing Clin Electrophysiol May 2005;28:372-377.

18. Zhang J, Sacher F, Hoffmayer K, et al. Cardiac electrophysiological substrate underlying the ECG phenotype and electrogram abnormalities in Brugada syndrome patients. Circulation Jun 2 2015;131:1950-1959.

19. Pannone L, Monaco C, Sorgente A, et al. High-density epicardial mapping in Brugada syndrome: Depolarization and repolarization abnormalities. Heart Rhythm Mar 2022;19:397-404.

20. Elliott MK, Strocchi M, Mehta VS, Wijesuriya N, Mannakkara NN, Jackson T, Pereira H, Behar JM, Bishop MJ, Niederer S, Rinaldi CA. Dispersion of repolarization increases with cardiac resynchronization therapy and is associated with left ventricular reverse remodeling. J Electrocardiol May-Jun 2022;72:120-127.

21. Huang Z, Patel C, Li W, Xie Q, Wu R, Zhang L, Tang R, Wan X, Ma Y, Zhen W, Gao L, Yan GX. Role of signal-averaged electrocardiograms in arrhythmic risk stratification of patients with Brugada syndrome: a prospective study. Heart Rhythm Aug 2009;6:1156-1162.

22. Ten Sande JN, Coronel R, Conrath CE, Driessen AH, de Groot JR, Tan HL, Nademanee K, Wilde AA, de Bakker JM, van Dessel PF. ST-Segment Elevation and Fractionated Electrograms in Brugada Syndrome Patients Arise From the Same Structurally Abnormal Subepicardial RVOT Area but Have a Different Mechanism. Circ Arrhythm Electrophysiol Dec 2015;8:1382-1392.

23. Hoogendijk MG, Potse M, Linnenbank AC, et al. Mechanism of right precordial ST-segment elevation in structural heart disease: excitation failure by current-to-load mismatch. Heart Rhythm 2010;7:238-248.

24. Franz MR, Bargheer K, Rafflenbeul W, Haverich A, Lichtlen PR. Monophasic action potential mapping in human subjects with normal electrocardiograms: direct evidence for the genesis of the T wave. Circulation 1987;75:379-386.

25. Nademanee K, Raju H, de Noronha SV, et al. Fibrosis, Connexin-43, and Conduction Abnormalities in the Brugada Syndrome. J Am Coll Cardiol Nov 3 2015;66:1976-1986.

26. Srinivasan NT, Orini M, Providencia R, Dhinoja MB, Lowe MD, Ahsan SY, Chow AW, Hunter RJ, Schilling RJ, Taggart P, Lambiase PD. Prolonged action potential duration and dynamic transmural action potential duration heterogeneity underlie vulnerability to ventricular tachycardia in patients undergoing ventricular tachycardia ablation. Europace Apr 1 2019;21:616-625.

27. Hoogendijk MG, Potse M, Vinet A, de Bakker JM, Coronel R. ST segment elevation by current-to-load mismatch: an experimental and computational study. Heart Rhythm Jan 2011;8:111-118.

28. Lambiase PD, Ahmed AK, Ciaccio EJ, Brugada R, Lizotte E, Chaubey S, Ben-Simon R, Chow AW, Lowe MD, McKenna WJ. High-density substrate mapping in Brugada

syndrome: combined role of conduction and repolarization heterogeneities in arrhythmogenesis. Circulation Jul 14 2009;120:106-117.

29. Haissaguerre M, Extramiana F, Hocini M, et al. Mapping and ablation of ventricular fibrillation associated with long-QT and Brugada syndromes. Circulation Aug 26 2003;108:925-928.

30. Ashino S, Watanabe I, Kofune M, Nagashima K, Ohkubo K, Okumura Y, Mano H, Nakai T, Kunimoto S, Kasamaki Y, Hirayama A. Effects of quinidine on the action potential duration restitution property in the right ventricular outflow tract in patients with brugada syndrome. Circ J 2011;75:2080-2086.

31. Marquez MF, Bonny A, Hernandez-Castillo E, De Sisti A, Gomez-Flores J, Nava S, Hidden-Lucet F, Iturralde P, Cardenas M, Tonet J. Long-term efficacy of low doses of quinidine on malignant arrhythmias in Brugada syndrome with an implantable cardioverter-defibrillator: a case series and literature review. Heart Rhythm Dec 2012;9:1995-2000.

32. Shen T, Yuan B, Geng J, Chen C, Zhou X, Shan Q. Low-Dose Quinidine Effectively Reduced Shocks in Brugada Syndrome Patients with an Implantable Cardioverter Defibrillator: A Chinese Case Series Report. Ann Noninvasive Electrocardiol Jan 2017;22:1-6.

33. Rodriguez-Manero M, Sacher F, de Asmundis C, et al. Monomorphic ventricular tachycardia in patients with Brugada syndrome: A multicenter retrospective study. Heart Rhythm Mar 2016;13:669-682.

34. Mazzanti A, Tenuta E, Marino M, et al. Efficacy and Limitations of Quinidine in Patients With Brugada Syndrome. Circulation: Arrhythmia and Electrophysiology 2019;12:e007143.

35. Pannone L, Monaco C, Sorgente A, et al. SCN5A mutation in Brugada syndrome is associated with substrate severity detected by electrocardiographic imaging and high-density electroanatomic mapping. Heart Rhythm Jun 2022;19:945-951.

36. Pereira H, Niederer S, Rinaldi CA. Electrocardiographic imaging for cardiac arrhythmias and resynchronization therapy. Europace Aug 5 2020;22:1447-1462.

TABLES

Table 1: Cohort Characteristics

	BrS Patients (n=12)
Male	11 (91.7)
Age (years)	47.6 ± 10.9
Body mass index	24.2 ± 2.1
Ethnicity	-
• North-West European	5 (41.7)
• North-East Asian	3 (25.0)
• Southern/Central Asian	3 (25.0)
• South-East Asian	1 (8.3)
Spontaneous type 1 ECG	11 (91.7)
History of cardiac arrest	3 (25.0)
History of syncope of unclear aetiology	2 (16.7)
Shanghai Score	4.6 ± 1.4
Family history of BrS	1 (8.3)
Family history of sudden cardiac death	1 (8.3)
Defibrillator *in situ*	4 (33.3)
Pathogenic or likely pathogenic *SCN5A* variant	2 (16.7)

Values are given as n (%) or mean ± SD.

Table 2. Non-invasive parameters at baseline and on-treatment

	Baseline	On-treatment	P-value
ECG			
Heart rate (bpm)	65.5 ± 7.5	65.3 ± 8.3	0.895
PR interval (ms)	180.6 ± 28.3	185.3 ± 22.5	0.239
QRS duration (ms)	110.7 ±16.1	117.8 ± 17.8	**0.004**
QT (ms)	378.3 ± 25.2	418.8 ± 32.8	**<0.001**
QTc (ms)	369.5 ± 26.0	434.8 ± 27.2	**<0.001**
Tpeak-Tend (ms)	90.7 ± 10.2	92.2 ± 15.6	0.790
Maximum J-point elevation (mV)	2.2 ± 1.1	2.1 ± 1.1	0.647
SAECG*			
Filtered QRS duration (ms)	112.1 ± 10.4	113.9 ± 9.9	0.567
Root mean squared voltage of terminal 40msec (μV)	19.1 ± 13.4	17.6 ± 10.1	0.722
Duration of terminal QRS <40μv (ms)	43.0 ± 11.3	44.8 ± 9.7	0.556
Number of patients with late potentials (%)	7 (63.6)	7 (63.6)	>0.999
ECGi			
Mean ST elevation BiV (mV)	0.4 ± 0.1	0.4 ± 0.1	0.214
Mean ST elevation RVOT (mV)	1.5 ± 0.7	1.8 ± 0.8	**<0.001**
Mean AT BiV (ms)	33.8 ± 6.3	35.4 ± 7.0	0.141
Mean AT RVOT (ms)	59.4 ± 13.5	63.8 ± 19.2	0.066
Mean AT RVOT-BIV (ms)	25.7 ± 10.7	28.3 ± 14.2	0.201
Activation gradient BiV (ms/mm)	0.5 ± 0.1	0.5 ± 0.1	0.087
Activation gradient RVOT (ms/mm)	1.1 ± 0.4	1.2 ± 0.6	0.150
Mean AT in late activated area (ms)	91.4 ± 11.4	101.1 ± 21.6	**0.043**
Mean RT BiV (ms)	258.2 ± 18.2	282.7 ± 24.3	**<0.001**
Mean RT RVOT (ms)	301.1 ± 24.1	348.8 ± 28.3	**<0.001**
Mean RT RVOT-BIV (ms)	42.9 ± 10.6	66.0 ± 13.0	**<0.001**
Repolarisation gradient BiV (ms/mm)	1.2 ± 0.4	1.9 ± 0.5	**<0.001**
Repolarisation gradient RVOT (ms/mm)	1.1 ± 0.4	1.6 ± 0.4	**<0.001**
T-wave amplitude BiV (mV)	0.48 ± 0.15	0.33 ± 0.10	**<0.001**
T-wave amplitude RVOT (mV)	0.97 ± 0.30	0.76 ± 0.23	**0.017**
T-wave width BiV (ms)	126.0 ± 7.5	152.0 ± 11.4	**<0.001**
T-wave width RVOT (ms)	138.6 ± 10.4	175.5 ± 7.2	**<0.001**
Mean ARI BiV (ms)	224.1 ± 14.7	247.0 ± 21.2	**0.001**
Mean ARI RVOT (ms)	241.3 ± 18.1	284.8 ± 21.5	**<0.001**
Mean ARI RVOT-BiV (ms)	17.2 ± 9.1	37.9 ± 12.6	**0.001**

Values are given as n (%) or mean ± SD.

*Patient DBR1 removed from SAECG analysis due to right bundle branch block.

Abbreviations: AT, activation time; ARI, activation-recovery interval; BiV, biventricular mass excluding RVOT; RT, repolarisation time; RVOT, right ventricular outflow tract.

FIGURE LEGEND

Figure 1: ST-segment elevation

ST-segment elevation was greater in the RVOT at baseline, with a statistically significant increase on-treatment. ECGi maps from a representative patient are presented in panel A, showing ST-segment elevation in mV at baseline and on-treatment, for entire BiV (left panel) and RVOT (right panel). Panel B shows comparative analysis of ST-segment elevation in the BiV (left panel) and RVOT (right panel) at baseline and on-treatment across the cohort.

Figure 2: Ventricular activation

Activation is delayed in RVOT at baseline with no significant change in the mean AT in the RVOT on-treatment. ECGi maps from a representative patient are presented in panel A, showing activation maps at baseline and on-treatment as well as maps of activation gradient, demonstrating a zone of wavefront deceleration into the RVOT at baseline and on-treatment. Panel B shows comparative analysis of mean activation time (left panel) and activation gradient (right panel) in the RVOT at baseline and on-treatment across the cohort.

Figure 3: Ventricular repolarisation

Repolarisation times were prolonged in the RVOT at baseline, with further delay on-treatment. ECGi maps from a representative patient are presented in panel A demonstrating a zone of steep repolarisation gradient in the region of the RVOT at baseline

and increasing on-treatment. Panel B shows analysis of mean repolarisation time (left panel) and repolarisation gradients (right panel) in the RVOT.

Figure 4: Activation-recovery intervals

The activation-recovery interval prolongs in the presence of Hydroquinidine. Panel A shows isochronal maps of activation-recovery interval from a representative patient at baseline and on-treatment. Panel B shows mean activation-recovery interval within the RVOT across the cohort.

Figure 5: Patient BEU6 developed monomorphic ventricular tachycardia on Hydroquinidine

12-lead Holter monitor tracing (with high praecordial lead placement) and ECGi maps at baseline and on-treatment for patient BEU6 who developed monomorphic ventricular tachycardia after starting Hydroquinidine.

Figure 6: Effect of Hydroquinidine in *SCN5A* (+) patients compared to *SCN5A* (-) patients

Results of analysis of ECGi at baseline and on-treatment with *SCN5A* (-) patients in grey and *SCN5A* (+) patients highlighted with BEU6 in red and CEE2 in orange. Activation maps for *SCN5A* (+) patients and a representative *SCN5A* (-) patient can be found in **Supplemental Figure 5**.

Abbreviations: ARI: activation-recovery interval; AT: activation time; EGM: electrogram; RT: repolarisation time; RVOT: right ventricular outflow tract.

Figure 1

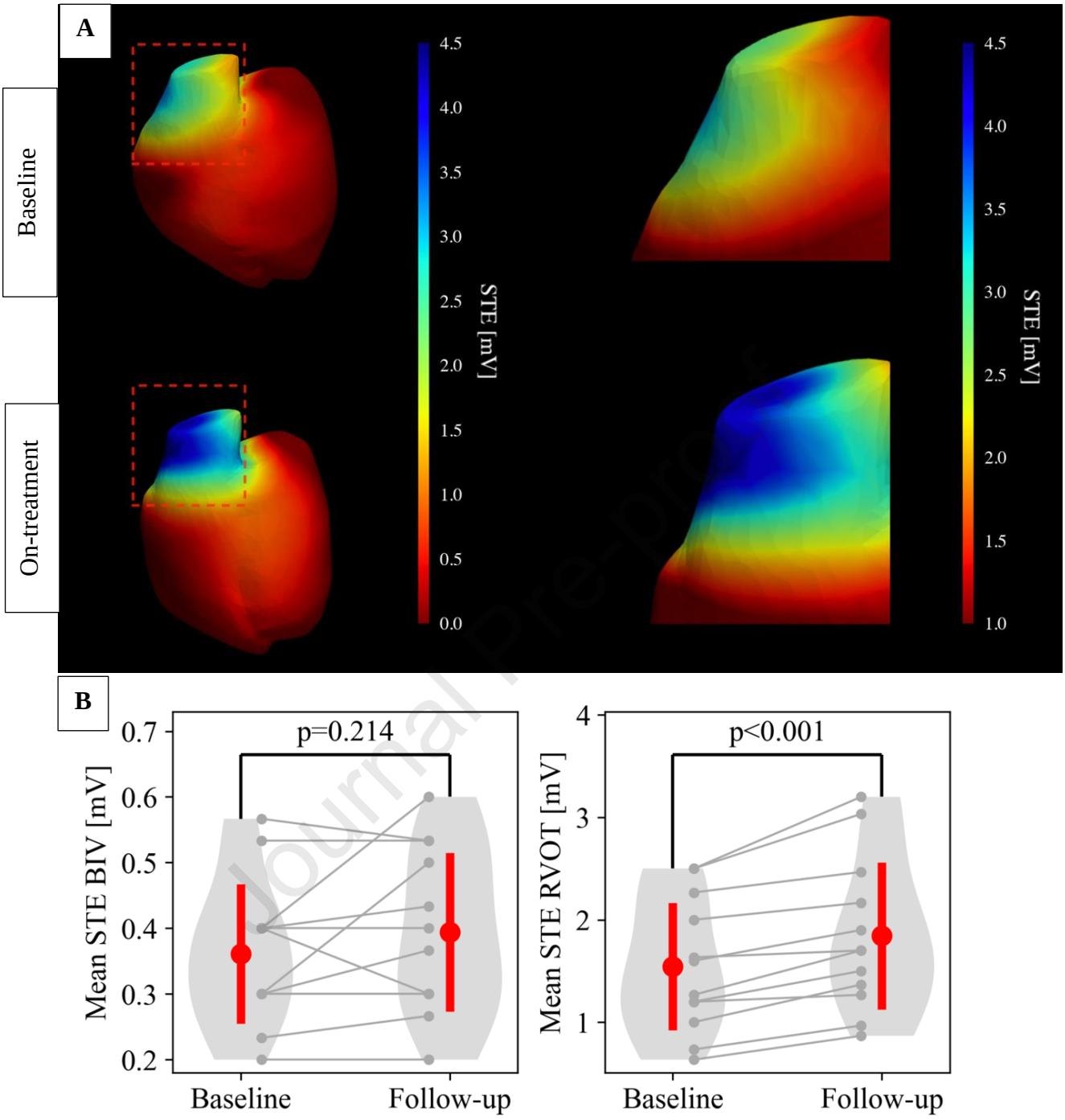

Figure 2

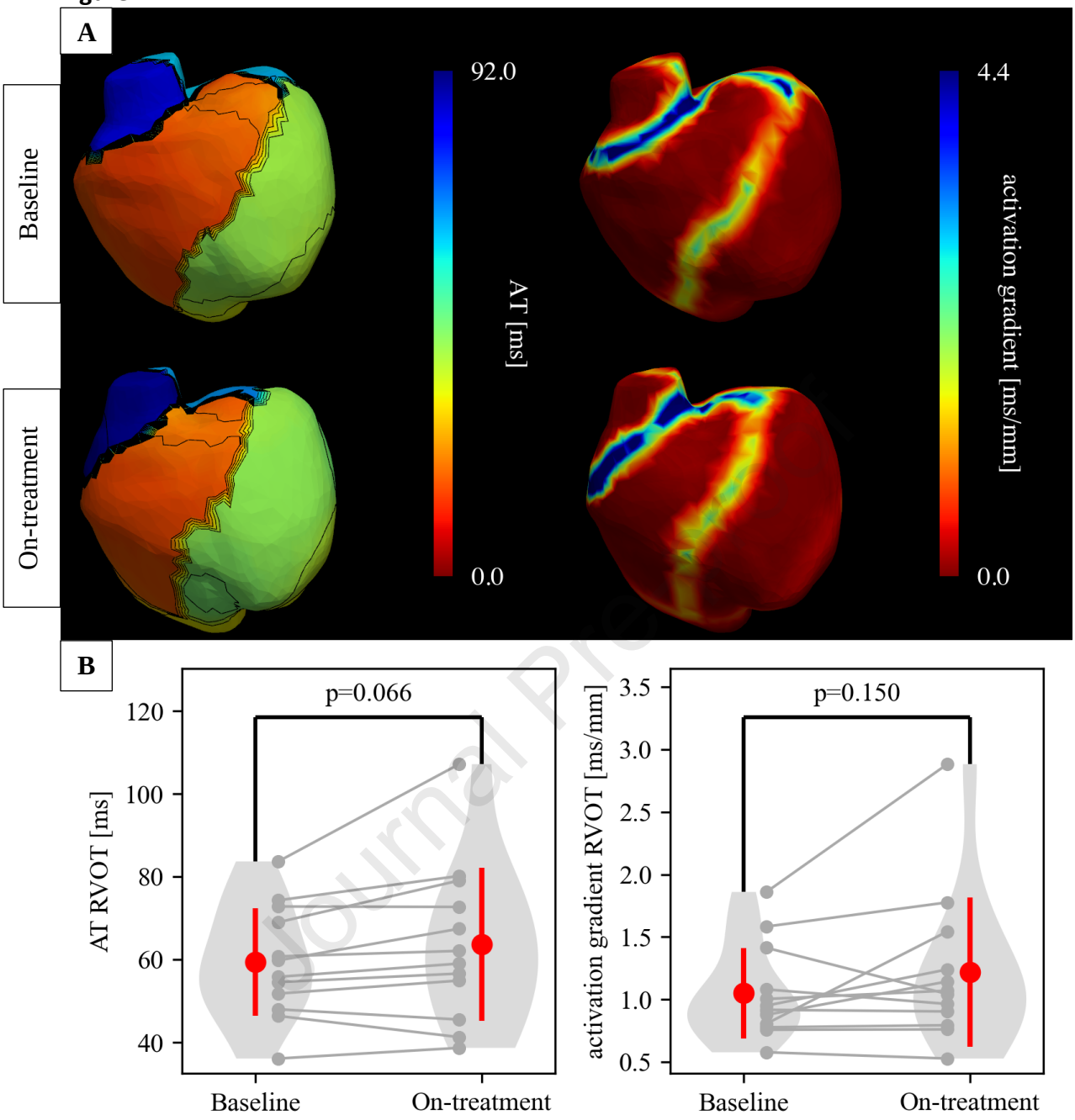
A
Baseline
On-treatment
92.0
AT [ms]
0.0
4.4
activation gradient [ms/mm]
0.0
B
p=0.066
AT RVOT [ms]
120
100
80
60
40
Baseline
On-treatment
p=0.150
activation gradient RVOT [ms/mm]
3.5
3.0
2.5
2.0
1.5
1.0
0.5
Baseline
On-treatment

Figure 3

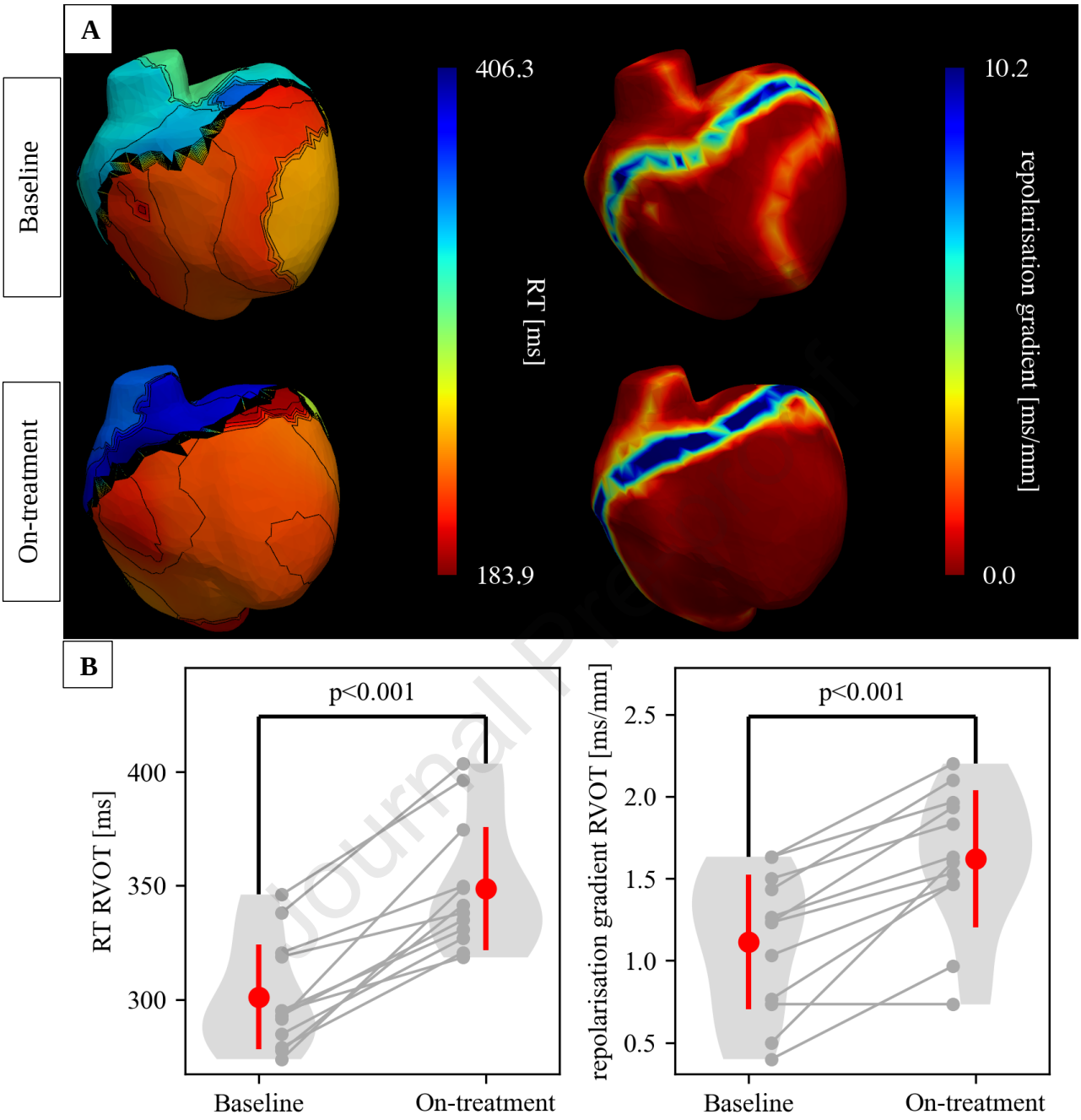
A
Baseline
On-treatment
406.3
183.9
RT [ms]
10.2
0.0
repolarisation gradient [ms/mm]
B
p<0.001
RT RVOT [ms]
400
350
300
Baseline
On-treatment
p<0.001
repolarisation gradient RVOT [ms/mm]
2.5
2.0
1.5
1.0
0.5
Baseline
On-treatment

Figure 4

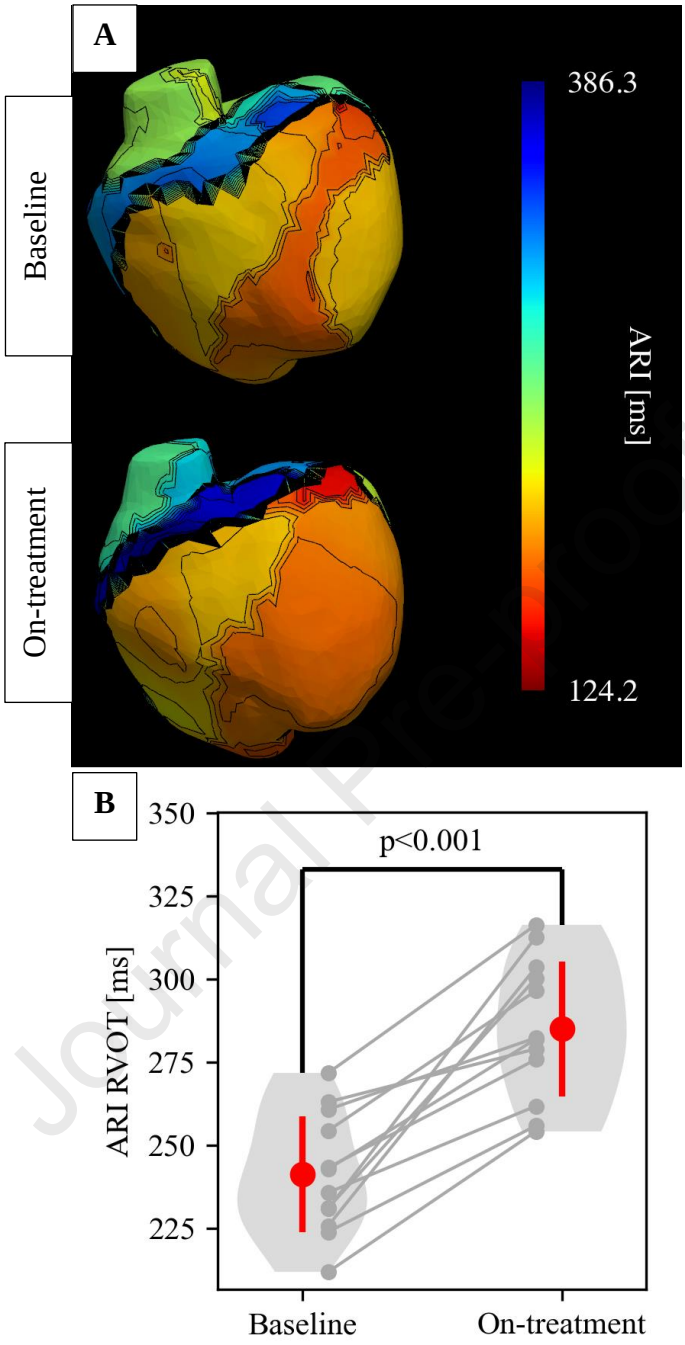

Figure 5

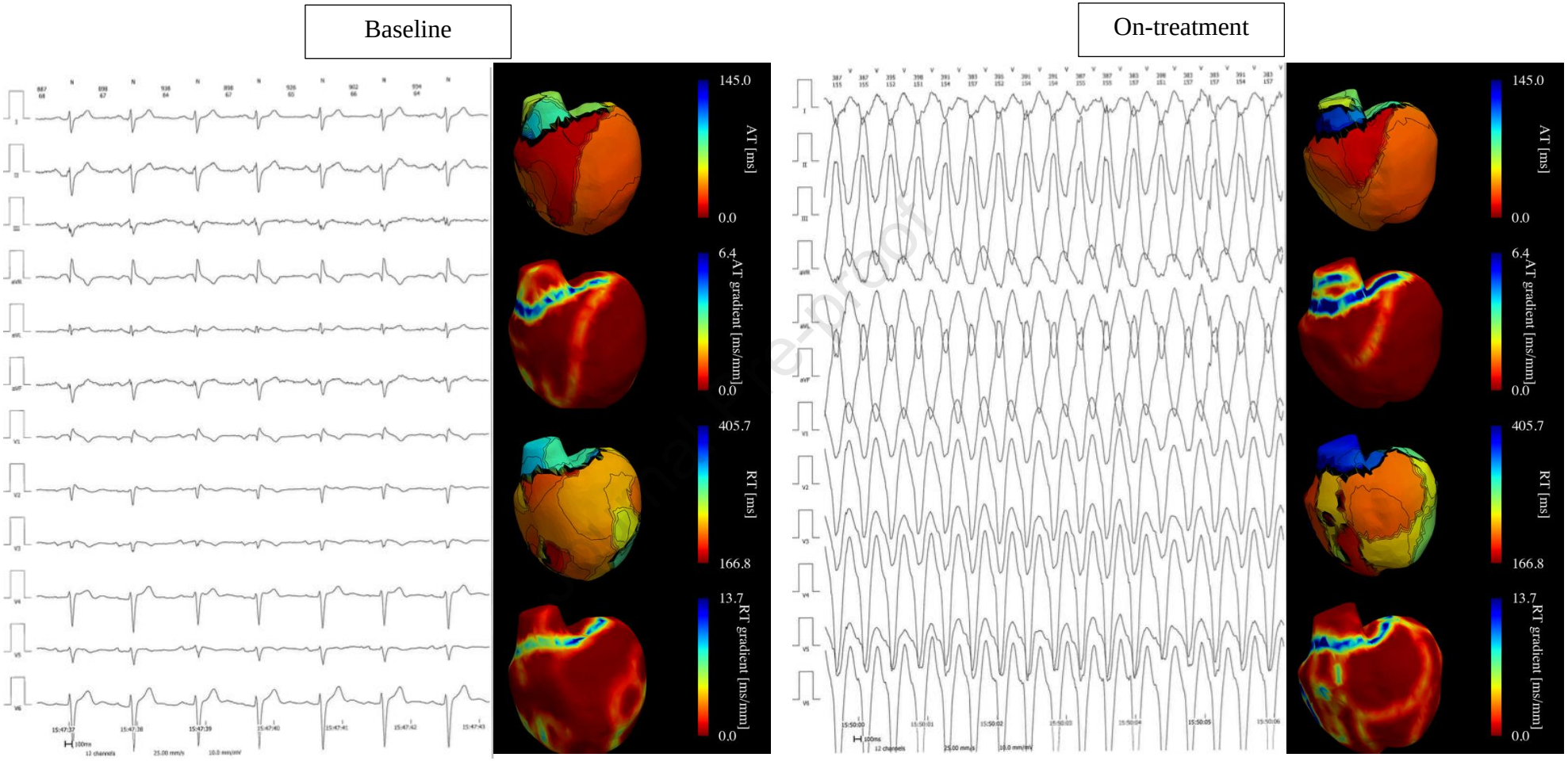
Baseline
On-treatment
145.0
AT [ms]
0.0
6.4
AT gradient [ms/mm]
0.0
405.7
RT [ms]
166.8
13.7
RT gradient [ms/mm]
0.0

Figure 6

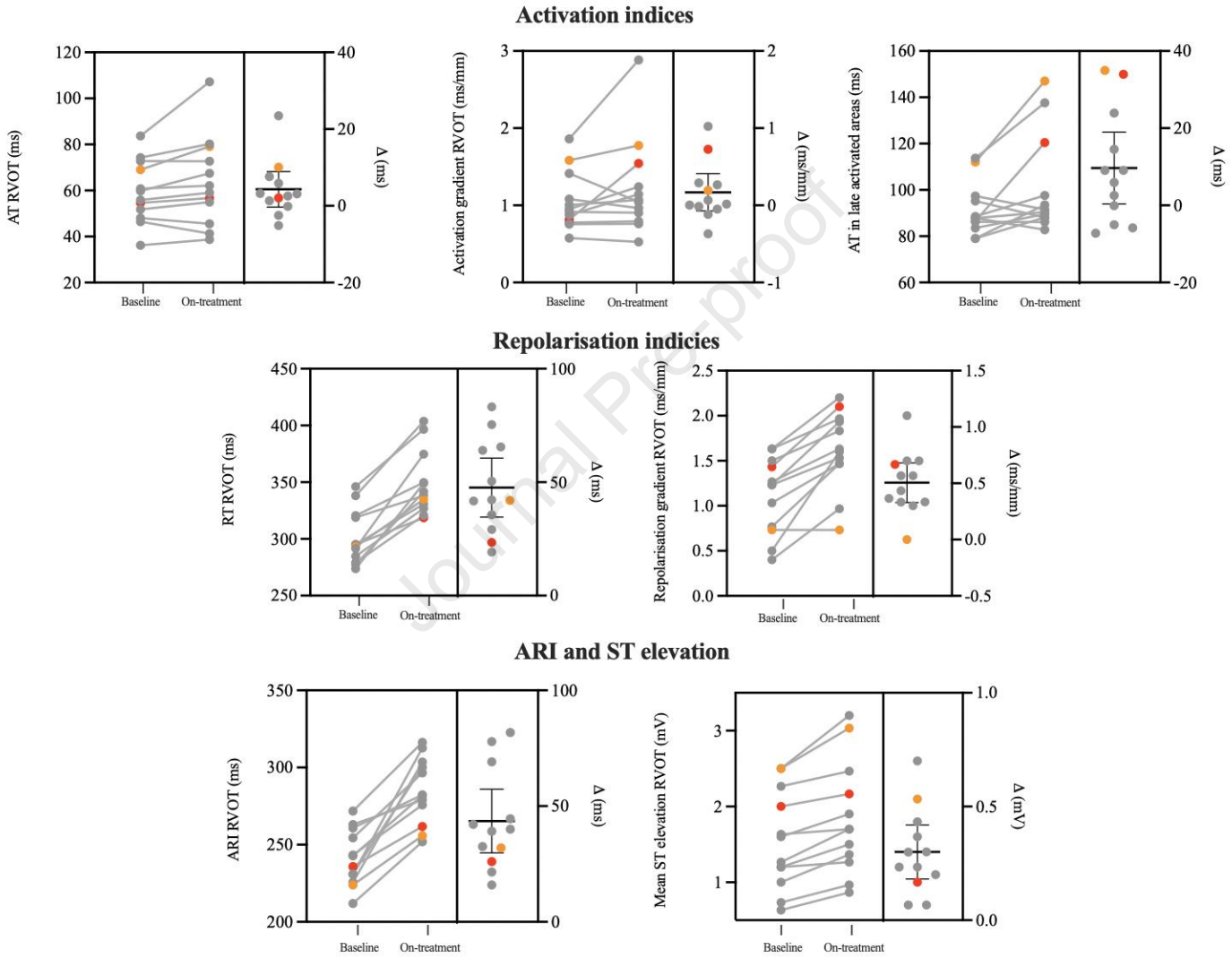

Figure 1

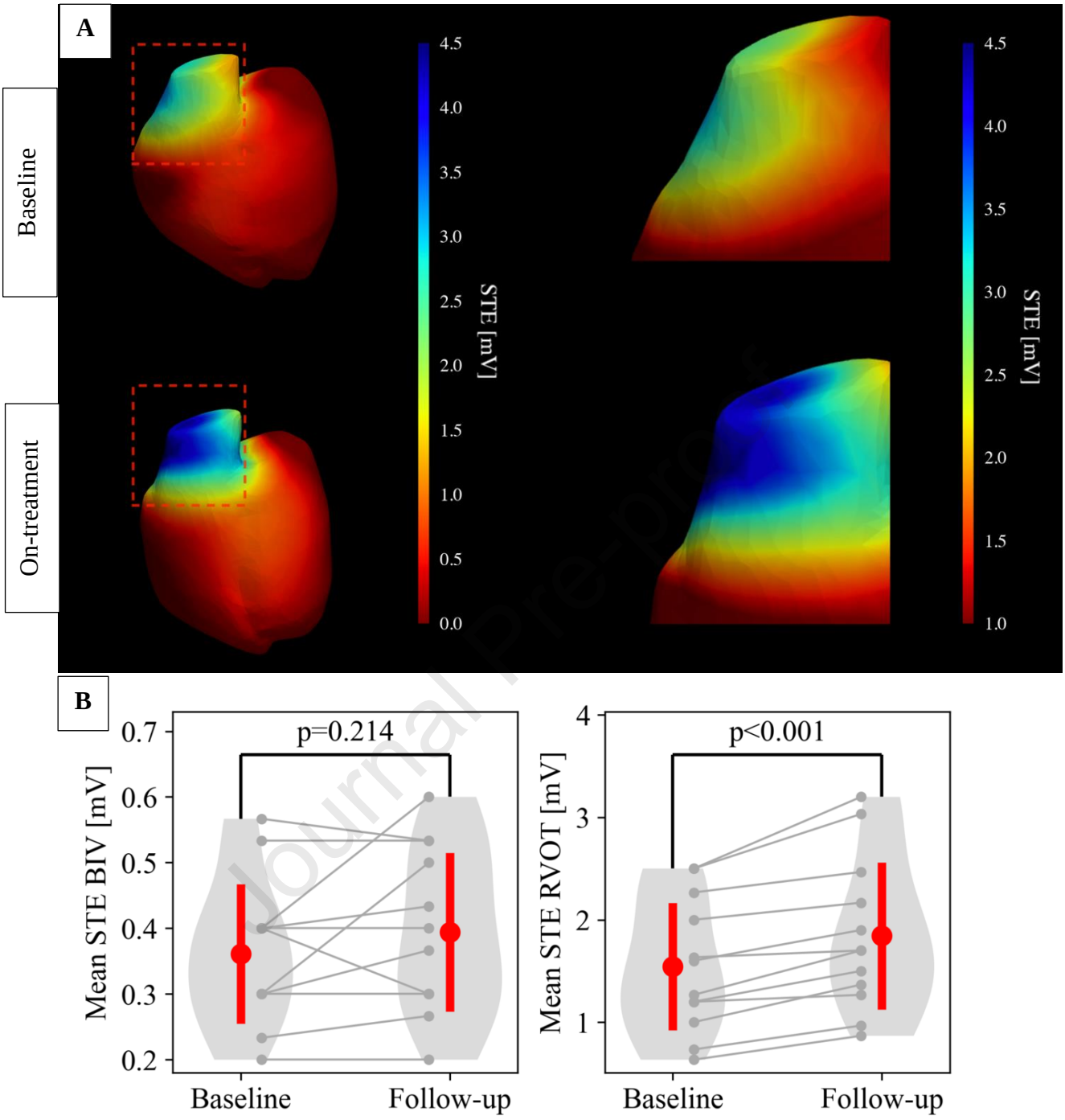

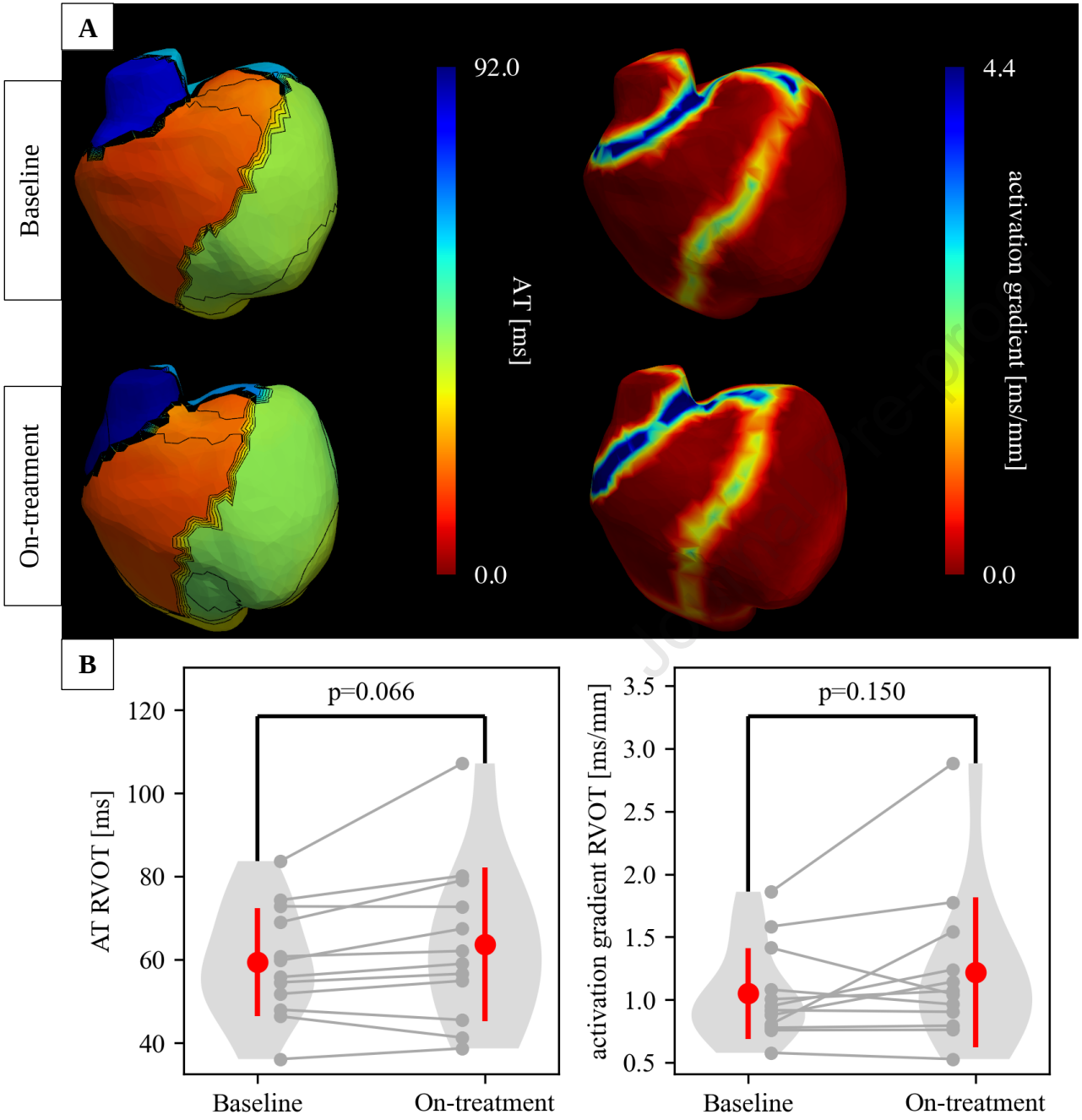
A
Baseline
On-treatment
92.0
AT [ms]
0.0
4.4
activation gradient [ms/mm]
0.0
B
p=0.066
AT RVOT [ms]
120
100
80
60
40
Baseline
On-treatment
p=0.150
activation gradient RVOT [ms/mm]
3.5
3.0
2.5
2.0
1.5
1.0
0.5
Baseline
On-treatment

Figure 3

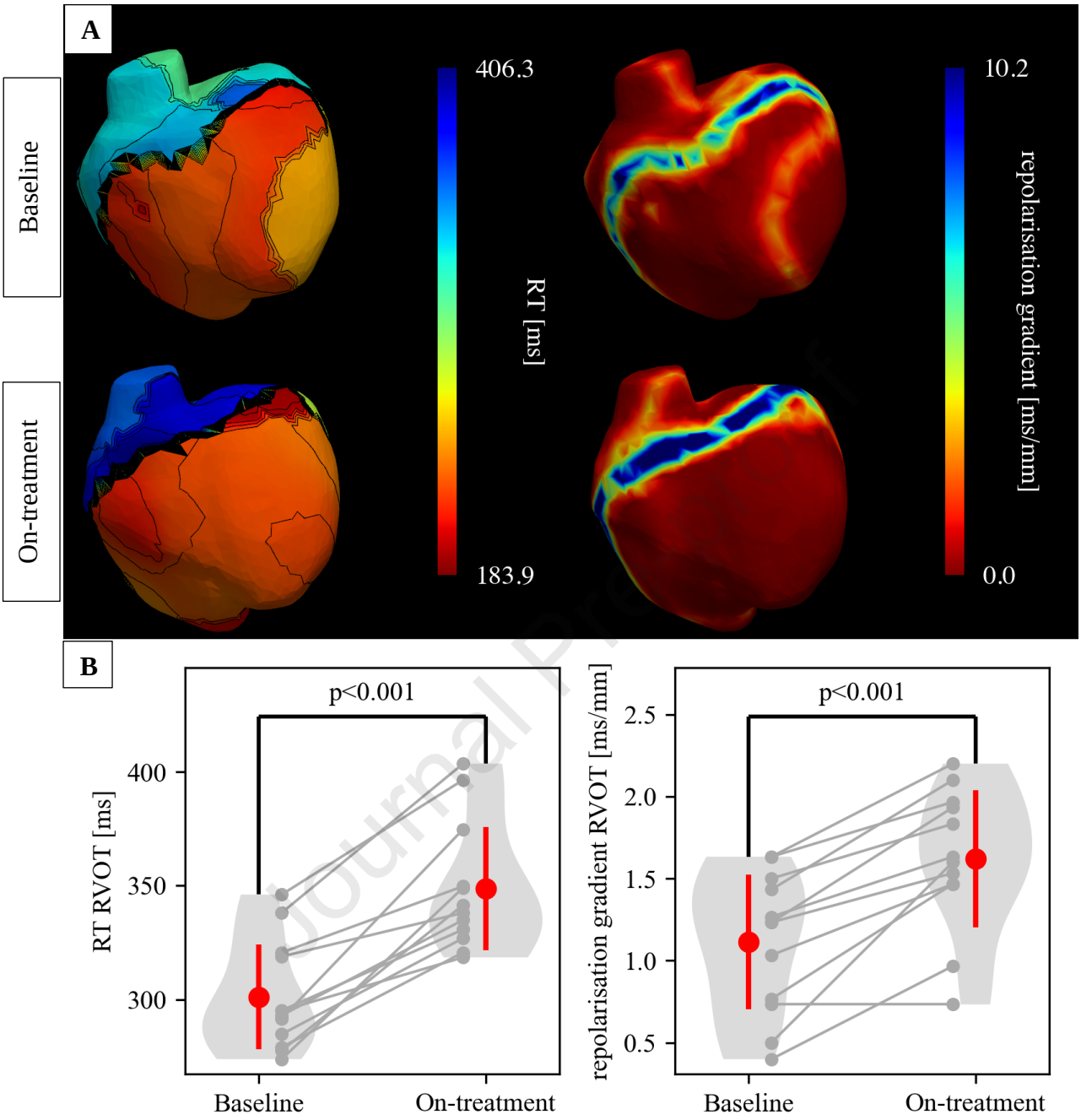
A
Baseline
On-treatment
406.3
183.9
RT [ms]
10.2
0.0
repolarisation gradient [ms/mm]
B
p<0.001
RT RVOT [ms]
400
350
300
Baseline
On-treatment
p<0.001
repolarisation gradient RVOT [ms/mm]
2.5
2.0
1.5
1.0
0.5
Baseline
On-treatment

Figure 4

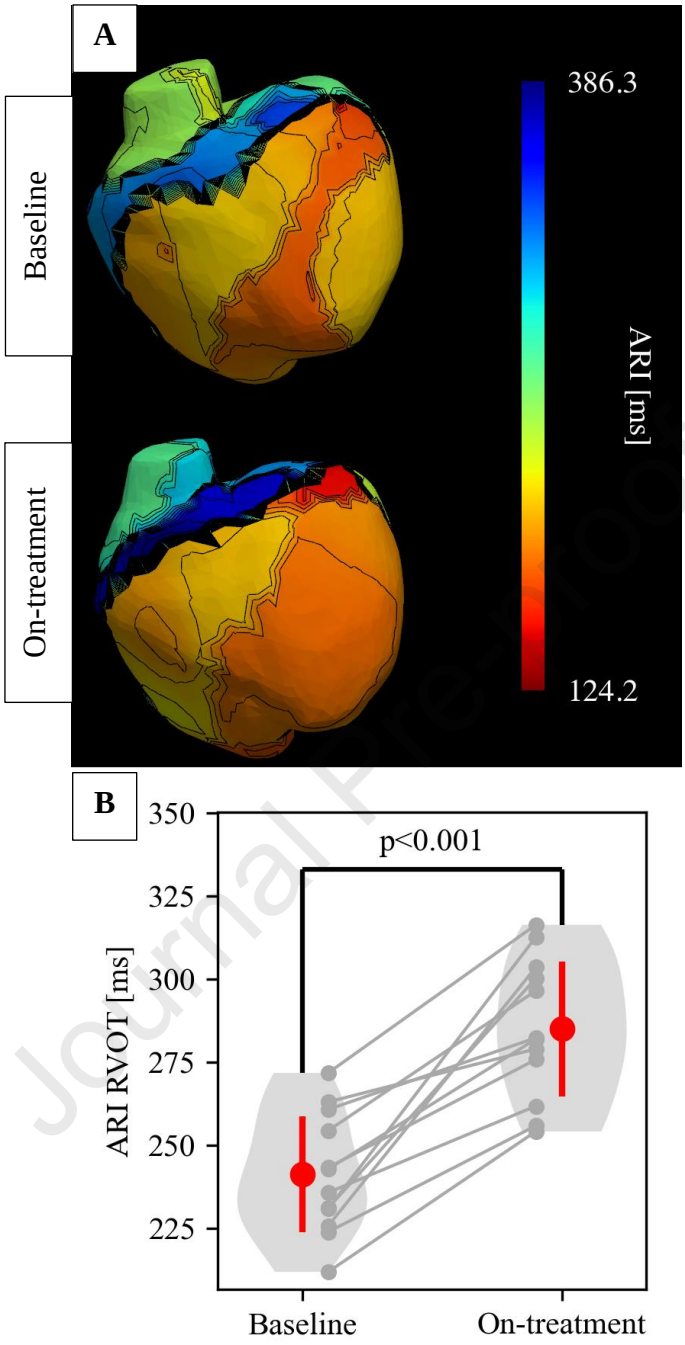

Figure 5

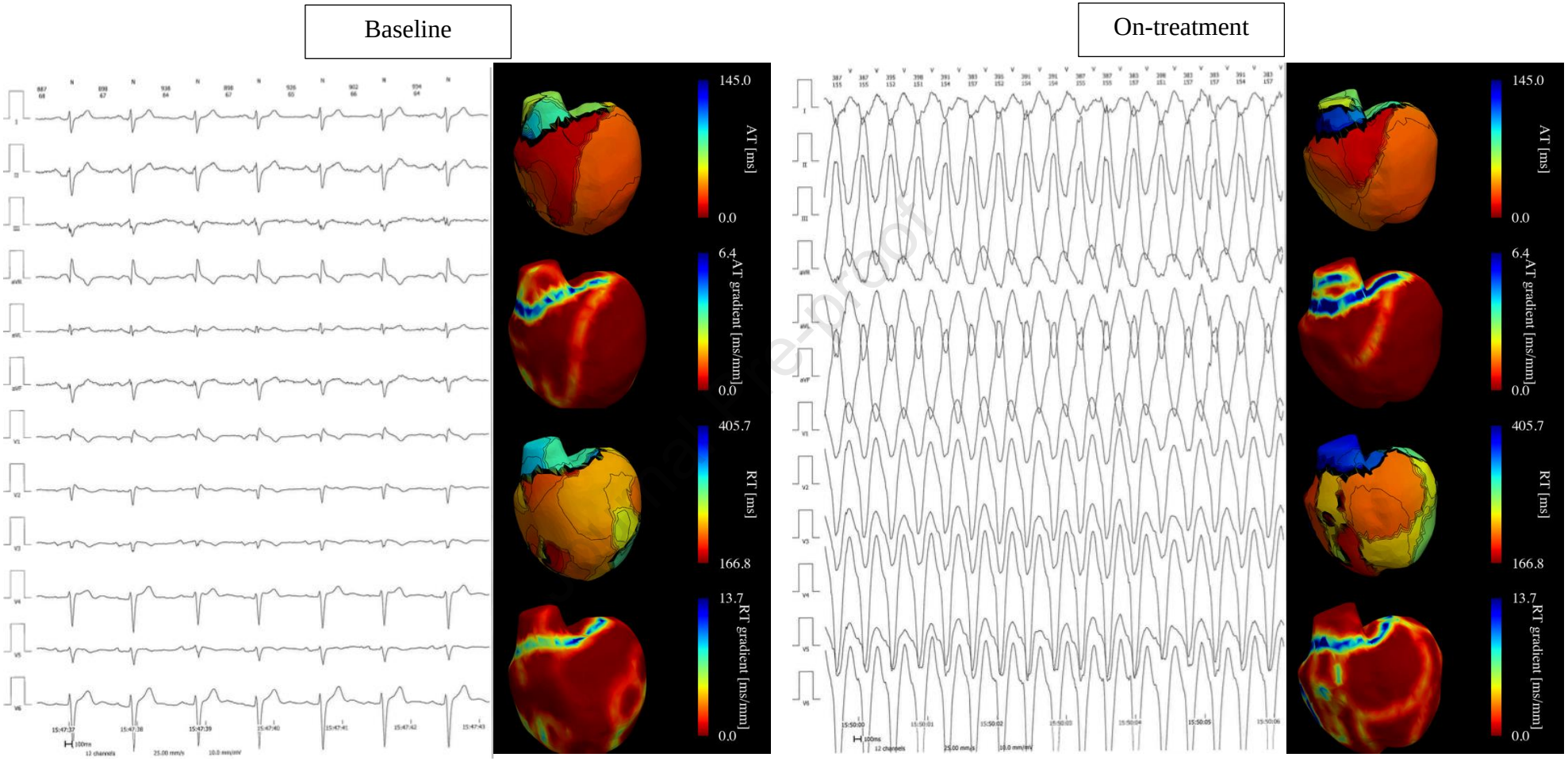
Baseline
On-treatment
145.0
AT [ms]
0.0
6.4
AT gradient [ms/mm]
0.0
405.7
RT [ms]
166.8
13.7
RT gradient [ms/mm]
0.0

Figure 6

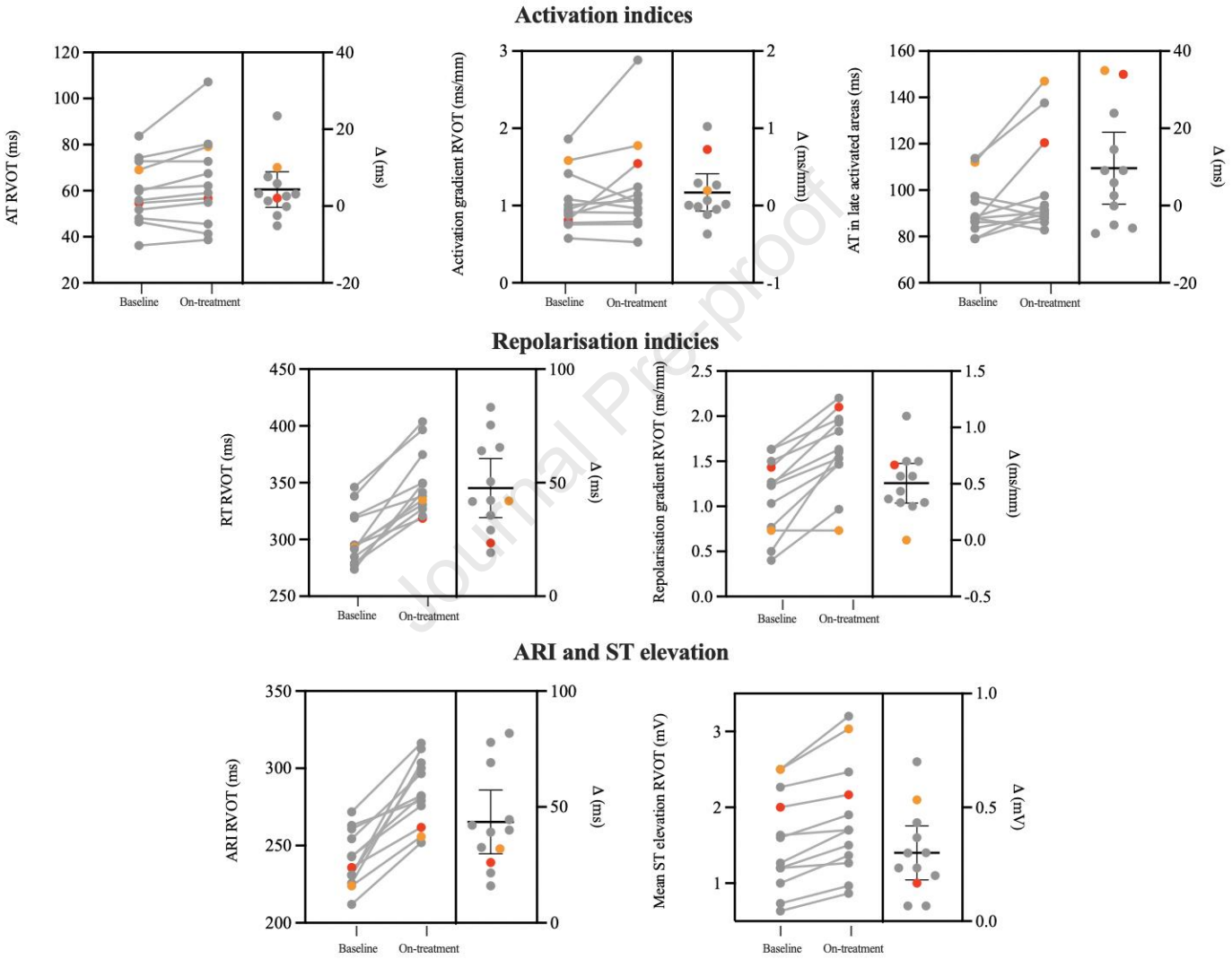

Supplemental Data

Supplemental Methods

Exclusion criteria:

- baseline QTc >450msec for men or > 460msec for women
- baseline QRS > 130msec
- baseline PR >230msec
- treatment with Quinidine for a clinical indication precluding drug free assessment
- treatment with a drug known to prolong QT interval
- treatment with a drug known to interact with Quinidine
- known hypersensitivity to Quinidine

Standard 12-lead, high position and signal averaged electrocardiogram

ECGs were recorded using the Mortara Eli 380 ECG machine. Heart rate, PR interval and QRS duration were determined from the standard 12-lead ECG by VERITAS® ECG interpretation algorithm. QT interval and Tpeak-Tend were measured manually on the standard 12-lead ECG using electronic calipers (EP Studios, Inc) by two independent physicians (JCI/RWS) and QT corrected for heart rate using Bazette's correction formula. Any discrepancy >20msec were adjudicated by an independent electrophysiologist (HR). ST segment elevation was analysed on the high lead placement ECG, measure using electronic calipers (EP Studios, Inc) and lead with maximal ST elevation was reported. SAECG were recorded and reported using Eli 350 Late Potential (Mortara) software.

Electrocardiographic imaging (ECGi)

Acquisition and map creation:

The 252-electrode CardioInsight™ Mapping Vest was applied to the prepared torso as per manufactures instructions. An ECG-gated computed tomography (CT) scan of the torso was performed with the vest *in situ*, ensuring field of view included all electrodes. Segmentation of the CT images was performed on the CardioInsight™ workstation to create a 3-dimensional shell of the heart. The superior margins of the segmentations were the pulmonary valve and aortic valves. To allow for focused assessment of the right ventricular outflow tract (RVOT), the aorta was not included in the epicardial shell. The atrioventricular valves were annotated to exclude signals at these locations and the left anterior descending artery tracked to delineate left and right ventricle on the epicardial shell.

Surface electrocardiograms from the 252-electrodes were acquired as the patient rested in the supine position. Beats for analysis were selected using the "Single Beat Mapping" interface and with a manually measured window of 50ms prior to QRS onset to 100ms post T-wave offset. Activation maps for a minimum of 3 consecutive beats were checked at each timepoint to ensure consistency. Maps were then exported for offline analysis.

ECGi Analysis:

Unipolar electrograms were reconstructed on the epicardial shell from body surface electrocardiogram recordings and CT-derived heart-torso geometry.

To analyse the results, we computed metrics for different regions of the ventricles.

We divided the ventricular nodes between the LV, the RV and the intra-ventricular septum by defining three landmarks to delineate the ventricular basal plane, two landmarks representing the LV-RV anterior and posterior junction points, and one landmark representing the apex. These landmarks were used to define planes dividing the ventricles following the direction of the left anterior descending (LAD) artery, with the septum defined to be a 1 cm-thick strip between the LV and the RV (Figure 1A). We also tagged an area within the RV to identify the RVOT as shown in Figure 1B, extending from the end of the RVOT to the closest point on the tricuspid valve ring.

Metrics were computed for:

- Right ventricular outflow tract (RVOT, orange area in Figure 1B)
- Biventricular region excluding the RVOT (BiV) region including the LV, the RV, the septum but excluding the RVOT (grey area in Figure 1B)

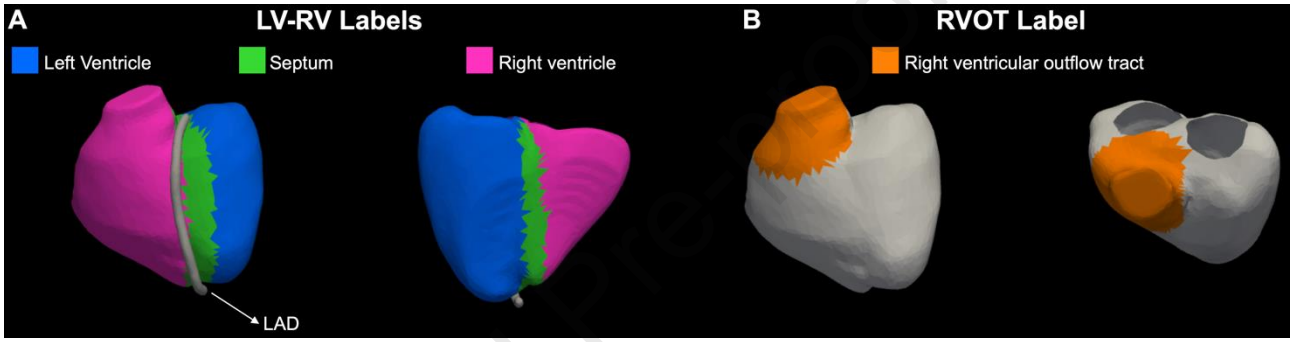

Figure 1 A Left and right ventricle labels. The left and the right ventricle are shown in blue and pink, while the intraventricular septum is shown in green. **B Right ventricular outflow tract label.** The ventricles are shown in grey, and the RVOT is highlighted in orange.

Analysis of ST-segment elevation:

ST-segment elevation was annotated automatically within a window of interest determined manually – opened at the J-point and closed at the isoelectric line.

Using the BiV and RVOT label, we computed the following metrics to compare ST-segment elevation between the RVOT and the rest of the ventricles (BiV):

- Mean ST-segment elevation BiV (excluding the RVOT) [mV]
- Mean ST-segment elevation RVOT [mV]

Analysis of ventricular activation:

Activation times (AT) were annotated at the steepest negative dV/dT of the last negative deflection in complex fractionated electrograms as reported previously in Brugada syndrome.[1] All activation times were shifted so that the earliest activation times coincided with 0 ms.

Using the BiV and RVOT label, we computed the following metrics to compare activation properties between the RVOT and the rest of the ventricles (BiV):

- Mean BiV activation time (excluding the RVOT) [ms]
- Mean RVOT activation time [ms]
- Difference between mean BiV and mean RVOT activation time [ms]

To investigate the distribution of areas of slow conduction, we computed the activation times gradient for each beat for each dataset. For each node, we considered the nodes within a 1 cm radius (along geodesic paths on the epicardial surface of the ventricles). We then computed the gradient as the mean ratio of the node-wise activation time difference and the distance between nodes (Figure 3A and B). This provided us with the local distribution of the activation time gradient over the epicardium of the ventricles, with high gradient areas showing areas of slow conduction or conduction block. To compare the conduction properties between datasets, we computed the following regional metrics within the same regions listed above:

- Mean BiV gradient (excluding the RVOT) [ms/mm]
- Mean RVOT gradient [ms/mm]

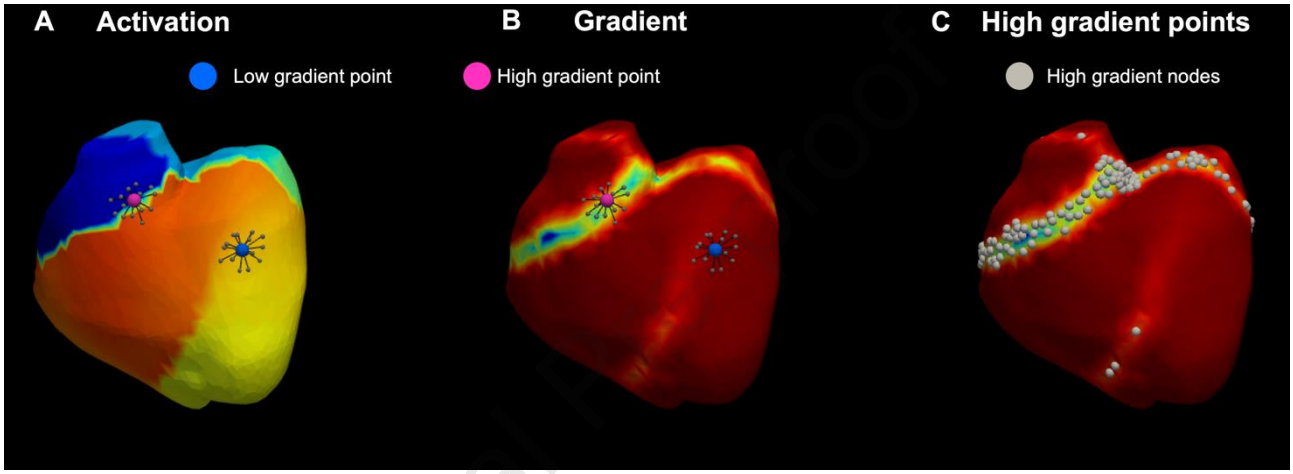

Figure 3 Activation times (**A**) and gradient distribution (**B**), highlighting two example points to show one low (blue) and one high (pink) gradient points. **C High gradient points.** Gradient map showing the high gradient nodes in grey, identified as the points with a gradient higher than the third quartile + three time the interquartile range.

Analysis of ventricular repolarisation:

Local repolarisation times (RT) were computed for each beat of each dataset with a custom Python code used in previous studies.[2] The ventricular electrograms were band-pass filtered between 0.5 and 20 Hz.[3] For each beat, we manually defined a window to isolate the T-wave for all electrograms. The local repolarisation time was computed as the time of maximum positive derivative during the T-wave. To exclude electrograms resulting in incorrect repolarisation time annotation, we removed outliers from the maps, defined as values greater than the 3rd quartile + 1.5 times the interquartile range (IQR) and less than the 1st quartile – 1.5 times the IQR. We also excluded signals with a T-wave amplitude below 0.05 mV. For the excluded points, we recomputed the local repolarisation times by interpolating the maps using an open-source code assuming no uncertainty on the known repolarisation times.[4] The repolarisation times were corrected for heart rate using the Fridericia formula.[5] Activation-recovery intervals (ARIs), a surrogate of local action-potential duration, were then computed as the difference between the corrected local repolarisation and local activation times (ARI = RT corrected for heart rate – AT). Figure 4 shows four example electrograms with annotated repolarisation times, together with the corresponding maps for the activation times, repolarisation times and ARIs.

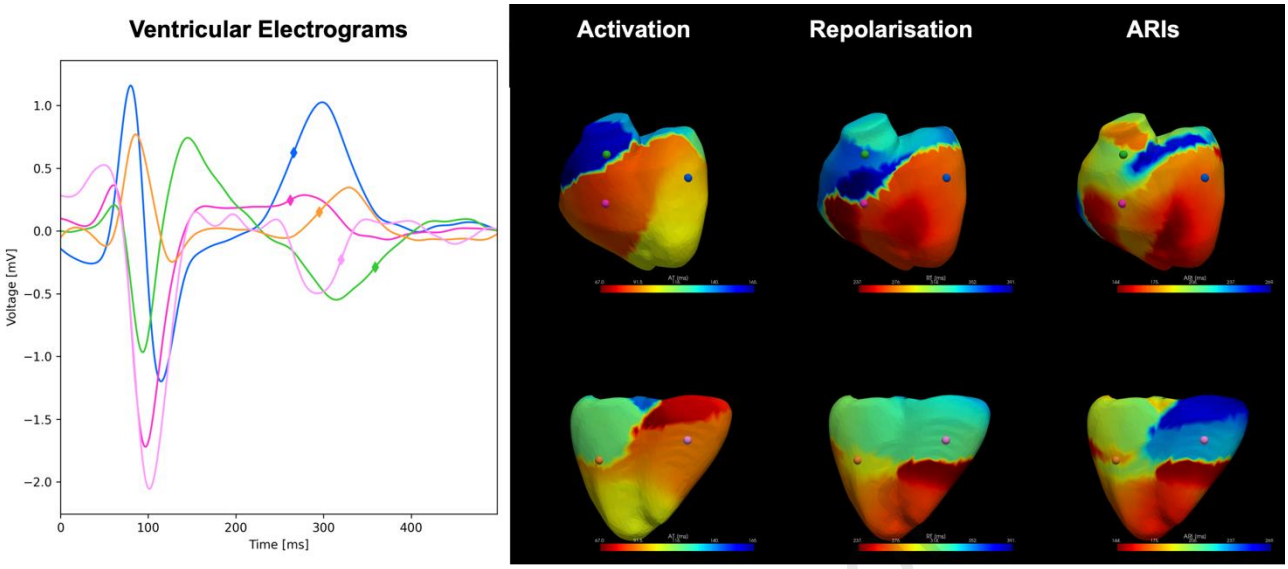

Figure 4 Repolarisation times computation. On the left, example filtered ventricular electrograms are shown, with diamonds indicating the annotated repolarisation times. The maps on the right show the local activation times, repolarisation times and activation-recovery intervals (ARIs). The points highlighted in the maps correspond to the location of the example electrograms shown on the left.

Using the regions described above, we computed regional repolarisation and ARI metrics to investigate local differences in repolarisation properties (corrected for heart rate). The following metrics were analysed:

- Mean BiV repolarisation time (excluding the RVOT) [ms]
- Mean RVOT repolarisation time [ms]
- Difference in mean repolarisation times between the RVOT and the rest of the ventricles [ms]

For the ARIs, the following metrics were computed:

- Mean BiV ARI [ms]
- Mean RVOT ARI [ms]
- Difference between mean BiV and mean RVOT ARI [ms]

We computed repolarisation gradients similarly to activation time gradients, using repolarisation times corrected for heart rate. We then computed the following metrics for repolarisation gradients:

- Mean BiV repolarisation gradient [ms/mm]
- Mean RVOT repolarisation gradient [ms/mm]

We also investigated changes in T-wave properties by computing the local T-wave amplitude and width. First, we filtered the ventricular electrograms with a band-pass filter between 0.5 and 20 Hz (same filtering used for repolarisation time annotation). Then, we identified the most prominent peak within a manually defined time window isolating the T-wave, and the amplitude and width of that peak were computed as shown in Figure 5. The T-wave widths were corrected for heart rate with the Fredericia formula for consistency with the heart rate correction used for repolarisation time. We computed the following metrics for T-wave properties:

- Mean T-wave amplitude in the ventricles excluding the RVOT [mV]
- Mean T-wave amplitude in the RVOT [mV]

- Mean T-wave width in the ventricles excluding the RVOT [ms]
- Mean T-wave width in the RVOT [ms]

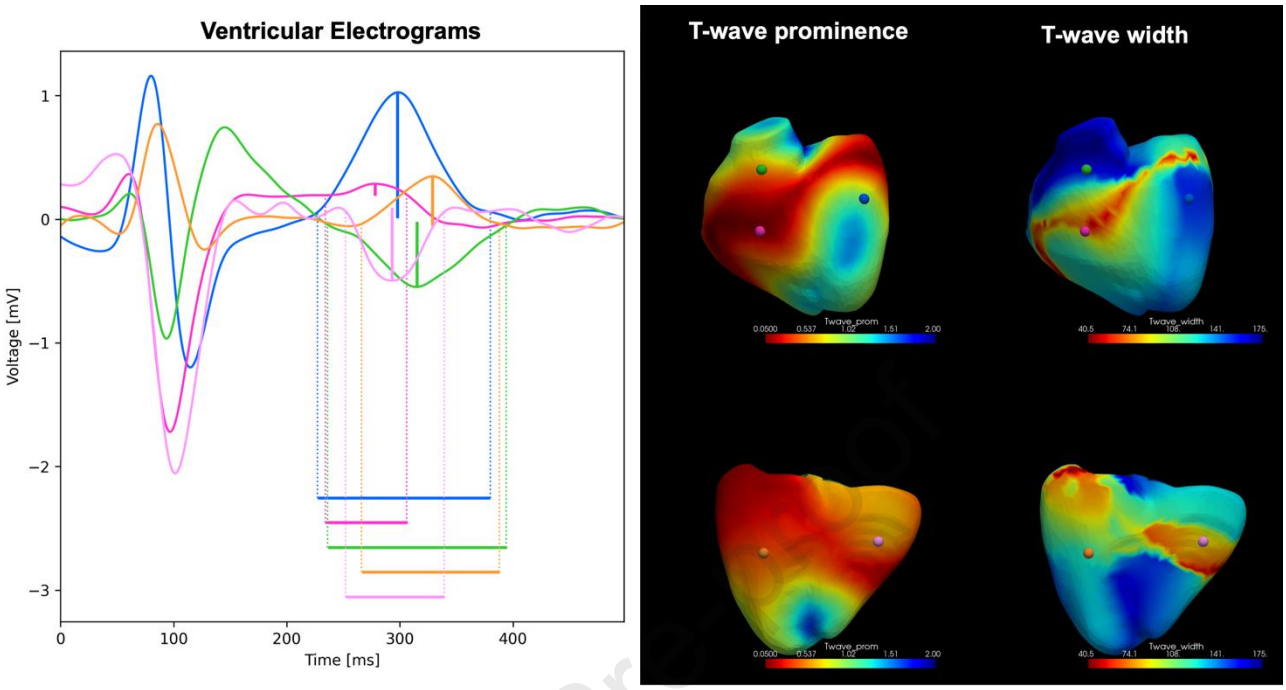

Figure 5 T-wave properties. On the left, example filtered ventricular electrograms are shown, with the solid vertical lines indicating the T-wave prominence, and the solid horizontal lines indicating the T-wave width. The maps on the right show the local T-wave prominence and width. The points highlighted in the maps correspond to the location of the example electrograms shown on the left.

Activation times were computed by Medtronic Inc using a proprietary analysis. Otherwise, analysis was carried out with custom code developed in Python3. Metrics are presented graphically with violin plots showing the density distribution of the data points, mean values and error bars depicting the standard deviation of the data.

Supplemental Tables

Supplemental Table 1: ECG, SAECG and ECGi parameters at baseline and on-treatment grouped by serum Hydroquinidine status.

	Therapeutic (N= 5)			Sub-therapeutic (N=7)			
	Baseline	On-treatment	P-value*	Baseline	On-treatment	P-value*	P-value**
ECG							
Heart rate (bpm)	68.0 ± 8.5	67.0 ± 10.7	0.808	63.7 ± 6.8	64.0 ± 6.8	0.883	0.748
PR interval (ms)	166.4 ± 17.6	177.2 ± 16.5	0.137	190.7 ± 31.1	191.1 ± 25.6	0.930	0.193
QRS duration (ms)	114.0 ± 20.6	117.6 ± 20.5	0.253	108.3 ± 13.25	117.9 ± 17.2	**0.008**	0.136
QT (ms)	379.6 ± 19.3	427.6 ± 33.4	**0.012**	377.3 ± 30.2	412.6 ± 33.5	**0.005**	0.360
QTc (ms)	409.6 ± 29.9	449.4 ± 31.6	**0.001**	387.1 ± 20.1	424.3 ± 19.4	**0.001**	0.765
Tpeak-Tend (ms)	92.4 ± 9.1	81.0 ± 11.1	0.172	89.4 ± 11.5	100.1 ± 13.6	0.136	**0.040**
Maximum J-point elevation (mV)	2.5 ± 0.6	1.7 ± 1.2	0.077	2.0 ± 1.4	2.3 ± 0.4	0.438	0.066
SAECG[#]							
Filtered QRS duration (ms)	110.8 ± 13.2	110.0 ± 5.5	0.890	112.9 ± 9.5	116.1 ± 11.5	0.456	0.558
Root mean square voltage of terminal 40msec (μV)	20.8 ± 10.0	18.5 ± 7.8	0.781	18.2 ± 9.7	17.1 ± 11.8	0.850	0.887
Duration of terminal QRS <40μv (ms)	43.3 ± 12.6	43.8 ± 11.2	0.933	42.9 ± 11.8	45.4 ± 9.7	0.526	0.757
ECGi							
Mean AT BiV (ms)	35.3 ± 9.8	37.8 ± 9.1	**0.0454**	32.8 ± 2.5	33.8 ± 5.2	0.5639	0.5590
Mean AT RVOT (ms)	61.3 ± 18.6	68.7 ± 26.0	0.1519	58.1 ± 9.9	60.3 ± 13.9	0.3226	0.7221
Mean AT RVOT-BiV (ms)	26.1 ± 12.2	30.9 ± 18.3	0.3282	25.4 ± 10.6	26.5 ± 11.7	0.4813	0.8488
Activation gradient BiV (ms/mm)	0.5 ± 0.0	0.5 ± 0.1	0.489	0.5 ± 0.1	0.5 ± 0.1	0.137	0.4096
Activation gradient RVOT (ms/mm)	1.0 ± 0.5	1.3 ± 0.9	0.2489	1.1 ± 0.3	1.2 ± 0.4	0.471	0.4804
Mean RT BiV (ms)	265.8 ± 21.1	301.8 ± 25.1	**0.0062**	252.8 ± 15.2	269.2 ± 12.1	**0.0077**	0.0638
Mean RT RVOT (ms)	310.0 ± 30.1	365.3 ± 37.9	**0.003**	294.8 ± 18.7	337.0 ± 11.4	**0.0018**	0.4449
Mean RT RVOT-BiV (ms)	44.2 ± 10.0	63.5 ± 13.4	**0.0061**	42.0 ± 11.8	67.8 ± 13.5	**0.0024**	0.3664

Repolarisation gradient BiV (ms/mm)	1.3 ± 0.3	2.1 ± 0.5	**0.0094**	1.2 ± 0.5	1.7 ± 0.5	**0.0009**	0.0549
Repolarisation gradient RVOT (ms/mm)	1.3 ± 0.5	1.9 ±0.3	**0.0115**	1.0 ± 0.4	1.4 ± 0.5	**0.0036**	0.6627
T-wave amplitude BiV (mV)	0.45 ± 0.05	0.31 ± 0.09	**0.020**	0.51 ± 0.19	0.34 ± 0.12	**0.0077**	0.7826
T-wave amplitude RVOT (mV)	0.87 ± 0.36	0.67 ± 0.21	0.2528	1.04 ± 0.26	0.82 ± 0.24	**0.0425**	0.9213
T-wave width BiV (ms)	129.7 ± 4.5	154.5 ± 13.5	**0.0073**	123.4 ± 8.4	150.1 ± 10.4	**0.0001**	0.4067
T-wave width RVOT (ms)	143.7 ± 12.2	179.2 ± 5.8	**0.0110**	134.9 ± 7.8	172.9 ± 7.3	**0.0002**	0.9734
Mean ARI BiV (ms)	230.5 ± 15.5	264.0 ± 16.6	**0.0092**	219.4 ± 13.2	234.9 ± 15.2	**0.0259**	0.0628
Mean ARI RVOT (ms)	248.6 ± 15.4	296.6 ± 18.0	**0.0052**	236.0 ± 19.2	276.4 ± 20.8	**0.0043**	0.5700
Mean ARI RVOT-BiV (ms)	18.1 ± 11.4	32.9 ± 10.5	0.0587	16.6 ± 8.0	41.5 ± 13.5	**0.0065**	0.2732

Abbreviations: AT, activation time; ARI, activation-recovery interval; BiV, biventricular mass excluding RVOT; ms, milliseconds; RT, repolarisation time; RVOT, right ventricular outflow tract.

*P-value compares baseline and on-treatment within group (paired t-test)

**P-value compares effect of Hydroquinidine between groups (mixed effects model)

DBR1 removed from SAECG analysis due to right bundle branch block.

Supplemental Table 2: Spatial resolution of ECGi and inter- surface electrode distance

	Mean ECGi epicardial resolution [mm]	Standard deviation of ECGi epicardial resolution [mm]	Mean distance between torso electrodes [mm]	Standard deviation of distance between torso electrodes [mm]
AON1 Baseline	4.4	1.8	37.2	4.9
AON1 On-treatment	4.5	1.8	37.1	5.1
BEU6 Baseline	5.1	1.8	37.3	5.1
BEU6 On-treatment	4.4	1.8	37.5	5
BPU1 Baseline	4.4	1.8	36.7	5.3
BPU1 On-treatment	4.4	1.8	37	4.7
BQD1 Baseline	4.2	1.8	36.9	5.3
BQD1 On-treatment	5.1	1.9	37.1	4.9
CBX1 Baseline	4.3	1.8	34.2	6
CBX1 On-treatment	4.2	1.7	34.4	5.7
CCL1 Baseline	4.4	1.8	37.3	5.3
CCL1 On-treatment	4.5	1.8	37	5.1
CEE2 Baseline	4.7	1.9	36.9	5.5
CEE2 On-treatment	4.7	1.8	37.6	5
CTU1 Baseline	4.8	1.9	37	5.3
CTU1 On-treatment	4.4	1.8	37.1	5.3
CZF1 Baseline	4.4	1.8	36.9	5.4
CZF1 On-treatment	4.5	1.8	37.3	5.2
DBM1 Baseline	4.4	1.8	37.2	4.9
DBM1 On-treatment	4.4	1.7	37.3	5
DBR1 Baseline	4.5	1.8	34.8	6.2
DBR1 On-treatment	4.7	1.8	34.9	6.1
DCF1 Baseline	4.5	1.8	33.3	6.8
DCF1 On-treatment	4.5	1.7	33.8	6.8
Mean	4.5		36.4	
Standard deviation	0.2		1.3	

Supplemental Figures

Figure Legend

Supplemental Figure 1: Study protocol

Supplemental Figure 2: Electrogram morphology and fractionation from areas of late activation in representative patients.
Representative electrograms from patients demonstrate variable EGM morphology between patients with and without fractionation but with no significant change in fractionation at baseline and on-treatment with Hydroquinidine. Each graph plots the 10 electrograms with the smallest QRS amplitude from late activated areas.

Supplemental Figure 3: T-wave morphology in RVOT
T-wave width increases, and T-wave amplitude decreases during treatment with Hydroquinidine. Panel A shows T-wave metrics in the RVOT for all patients. Panels B shows T-wave morphology on EGMs from a representative patient at baseline (orange) and on-treatment (blue). T-wave morphology on praecordial ECG leads reconstructed from ECGi body surface signals are depicted in **Supplemental Figure 4**.

Supplemental Figure 4: Reconstruction of surface ECG from ECGi to demonstrate T-wave change with Hydroquinidine.
Representative case (BPU1) demonstrating T-wave flattening and increased T-wave width during Hydroquinidine therapy. ECG reconstructed from ECGi and lead selection indicated in lower panel.

Supplemental Figure 5: AT and activation gradient maps for representative patient, SCN5A negative patient (DBM1) and two patients with pathogenic SCN5A variants (BEU6 and CEE1)
Region of late activation within the RVOT appears to increase more in BEU6 and CEE2 compared to representative SCN5A negative patient DBM1.

Supplemental Figure 1

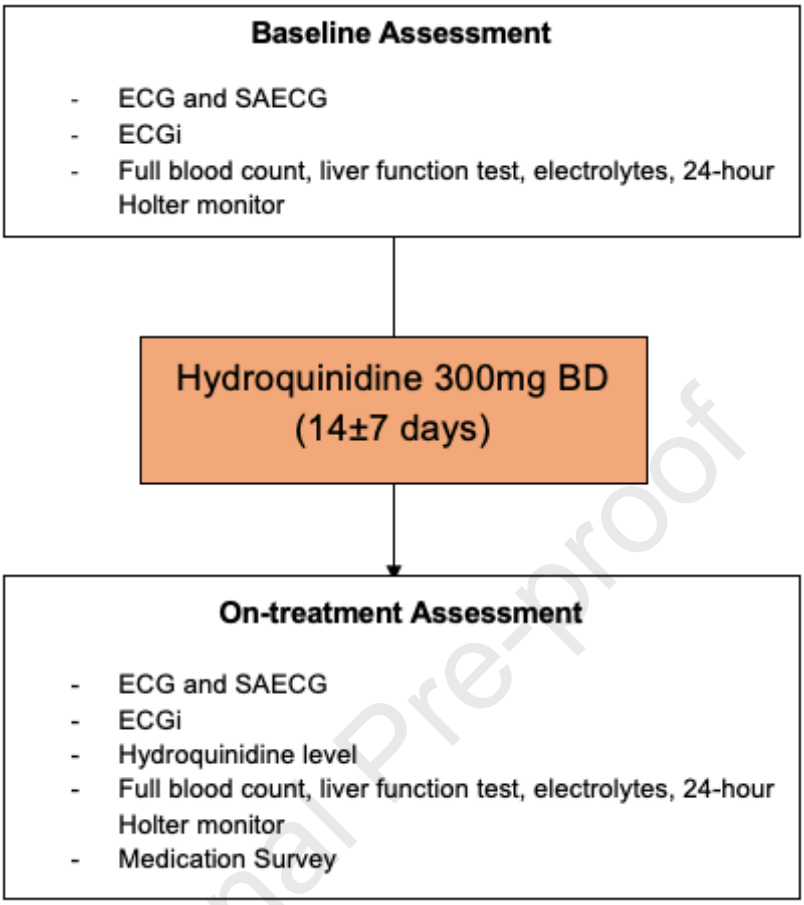

Supplemental Figure 2

	Baseline	On-treatment
DBM1	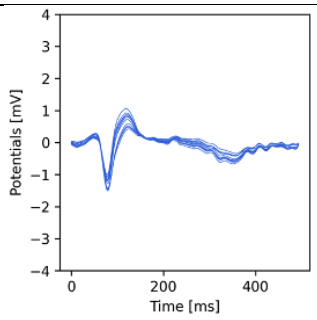	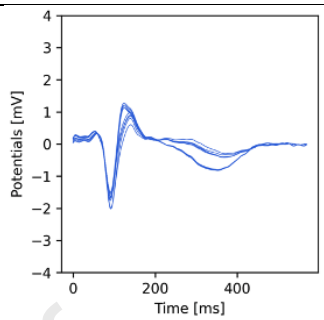
CEE2	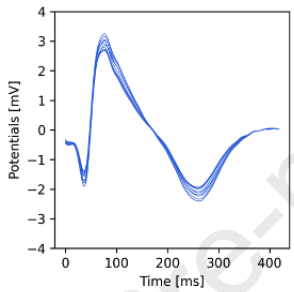	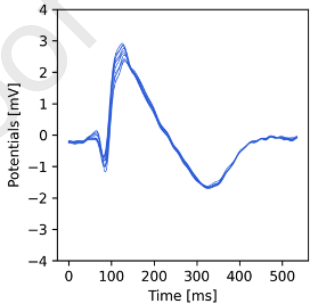
BQD1	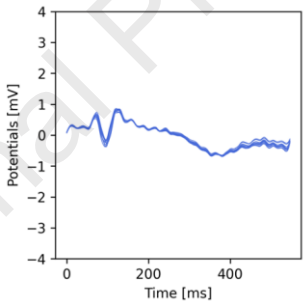	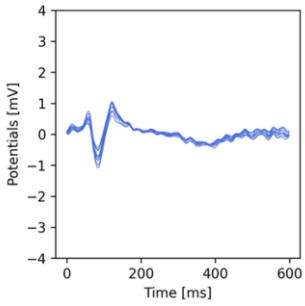
CZF1	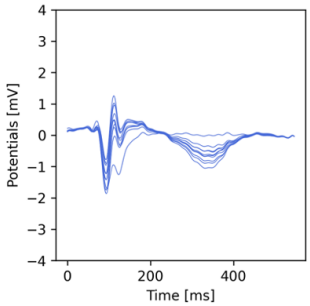	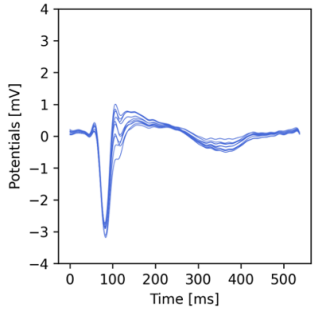
DBR1	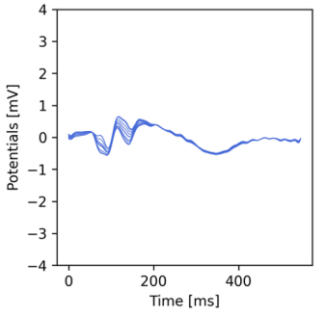	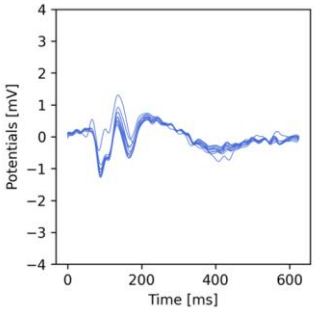

Supplemental Figure 3

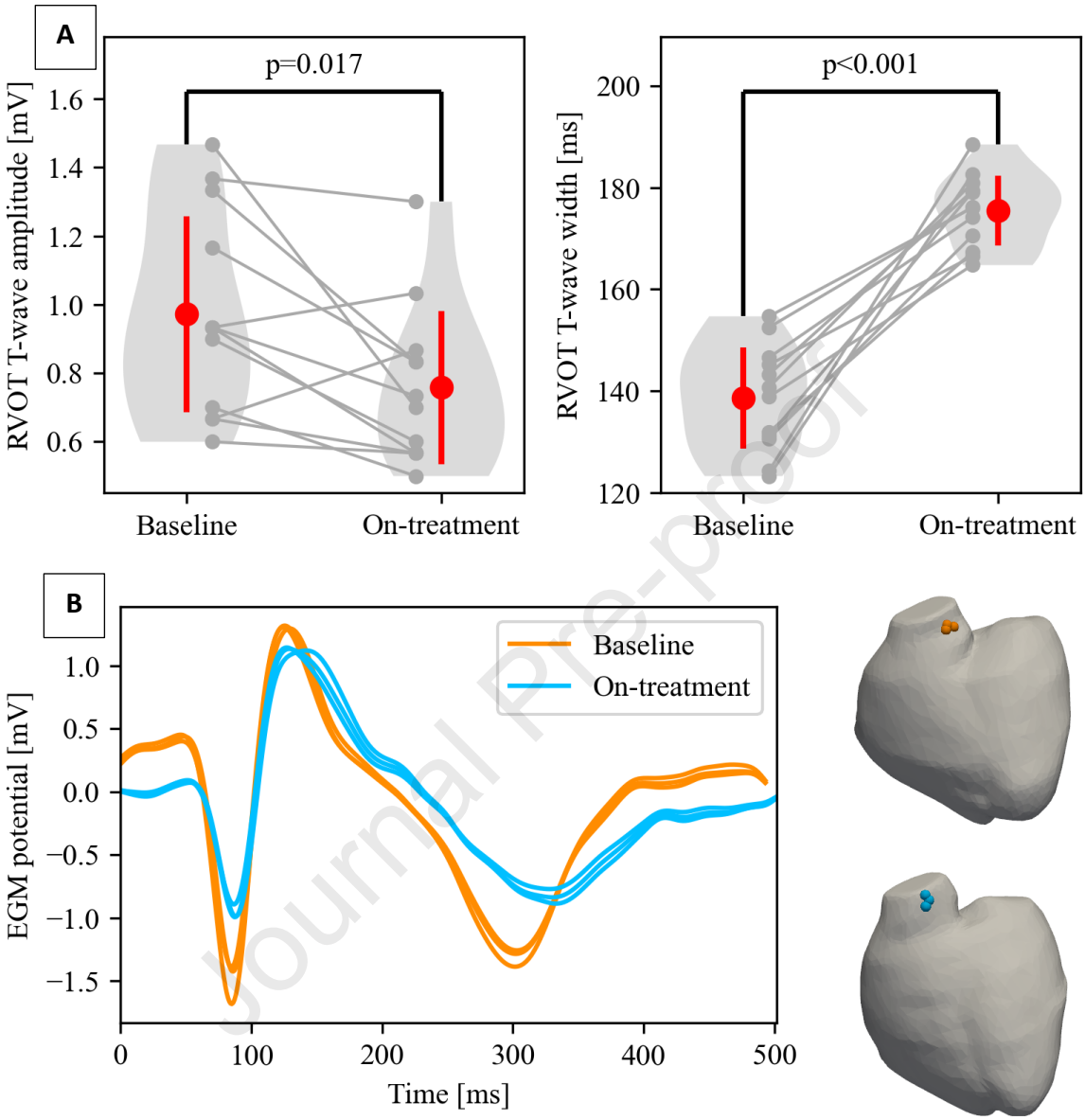

Supplemental Figure 4

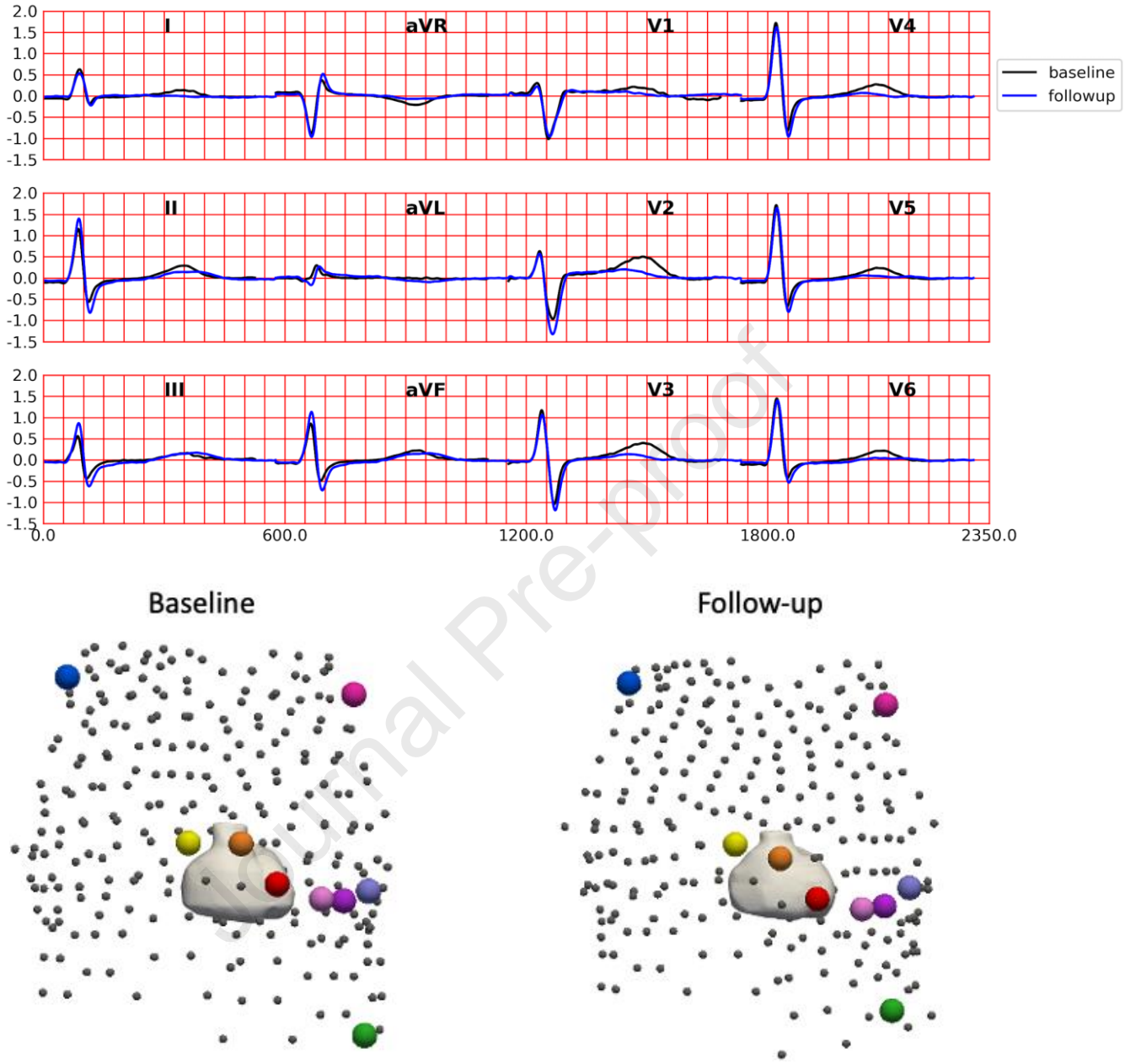

Supplemental Figure 5

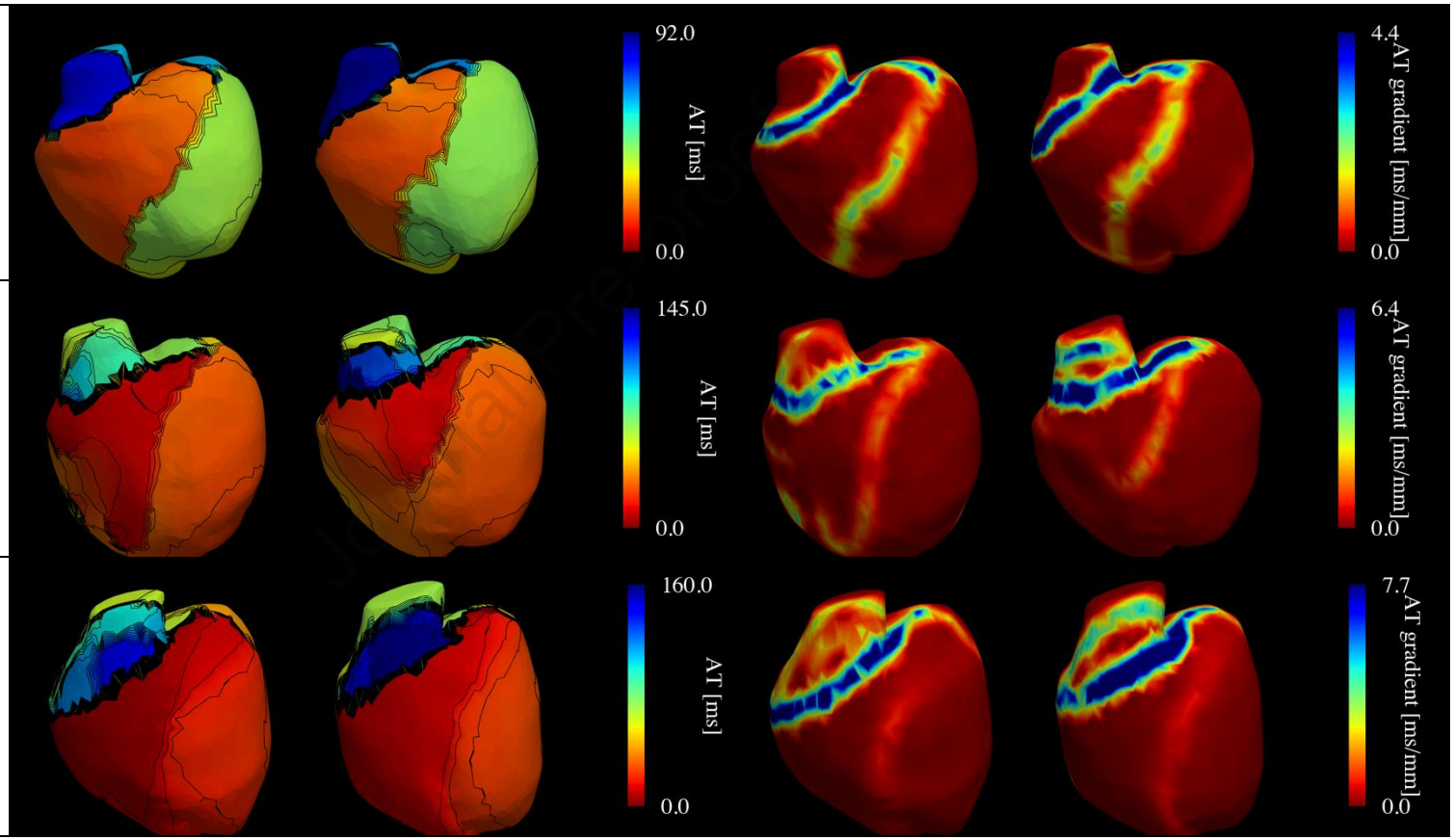

References

1. Nademanee K, Veerakul G, Nogami A, Lou Q, Hocini M, Coronel R, Behr ER, Wilde A, Boukens BJ, Haissaguerre M. Mechanism of the effects of sodium channel blockade on the arrhythmogenic substrate of Brugada syndrome. Heart Rhythm Mar 2022;19:407-416.

2. Elliott MK, Strocchi M, Mehta VS, Wijesuriya N, Mannakkara NN, Jackson T, Pereira H, Behar JM, Bishop MJ, Niederer S, Rinaldi CA. Dispersion of repolarization increases with cardiac resynchronization therapy and is associated with left ventricular reverse remodeling. J Electrocardiol May-Jun 2022;72:120-127.

3. Graham AJ, Orini M, Zacur E, et al. Simultaneous Comparison of Electrocardiographic Imaging and Epicardial Contact Mapping in Structural Heart Disease. Circ Arrhythm Electrophysiol Apr 2019;12:e007120.

4. Coveney S, Corrado C, Roney CH, O'Hare D, Williams SE, O'Neill MD, Niederer SA, Clayton RH, Oakley JE, Wilkinson RD. Gaussian process manifold interpolation for probabilistic atrial activation maps and uncertain conduction velocity. Philos Trans A Math Phys Eng Sci Jun 12 2020;378:20190345.

5. Orini M, Graham AJ, Martinez-Naharro A, Andrews CM, de Marvao A, Statton B, Cook SA, O'Regan DP, Hawkins PN, Rudy Y, Fontana M, Lambiase PD. Noninvasive Mapping of the Electrophysiological Substrate in Cardiac Amyloidosis and Its Relationship to Structural Abnormalities. J Am Heart Assoc Sep 17 2019;8:e012097.